

https://dspace.org/

The impact of Isomukaadial acetate on Plasmodium falciparum transcriptional gene regulation

N Salomane; T Mafuna; F Allie; Jabu Mahlangu; Robyn Van Zyl ...

https://hdl.handle.net/10539/48191
WOS

Downloaded from a DSpace repository. https://dspace.org/

scientific reports

Check for updates

OPEN

The impact of Iso-mukaadial acetate on *Plasmodium falciparum* transcriptional gene regulation

Nicolaas Salomane[1], Thendo Mafuna[1], Farhahna Allie[1], Jabu Sam Mahlangu[2,3], Robyn Lyenne van Zyl[2,3], Ofentse Pooe[4] & Mthokozisi Simelane[1]✉

Malaria remains prevalent globally despite various intervention strategies aimed at preventing its transmission. With the decreasing effectiveness of antimalarial drugs, medicinal plant extracts have been proposed as alternatives. Iso-mukaadial acetate extracted from *Warburgia salutaris* has shown anti-plasmodial activity, but the mechanism of inhibition is unknown. In this study, RNA sequencing analysis of *P. falciparum* NF54 strain treated with IMA was conducted to determine the possible targets of IMA. The expression profiles of *P. falciparum* genes regulated by IMA and chloroquine (antimalarial control) during the intraerythrocytic stage were analyzed with gene ontology tools, including PlasmoDB, ShinyGO and g: Profiler. IMA and chloroquine upregulated genes linked to parasite biological processes and cell adhesion molecular binding functions, including *Pf*EMP1, RIFIN, and STEVOR. Chloroquine specifically downregulated DNA replication processes involving DNA replication licensing factors MCM3 and DNA helicase, while IMA downregulated peptidyl-proline modification and glycolytic pathways. KEGG analysis suggested glycolysis-gluconeogenesis and pentose phosphate pathway enzymes (e.g., glyceraldehyde-3-phosphate dehydrogenase (GAPDH) and glucose-6-phosphate dehydrogenase (G6PD)-6-phosphogluconolactonase) as theoretical IMA targets, whose suppression could hypothetically reduce ATP and NADPH production, weakening parasite energy supply and antioxidant defenses. The inhibition of DNA replication components (MCM complex, DNA topoisomerases) by IMA, and the downregulation of DNA replication/repair proteins by chloroquine, may both impair genome integrity, contributing to the observed anti-plasmodial effects. IMA treatment was assumed to be associated with impairment of parasite energy metabolism, redox balance and DNA replication machinery. These effects differ from chloroquine, which primarily targeted DNA replication and repair processes, yet both drugs upregulated adhesion-associated gene families. Changes in the expression of metabolic and replication genes induced by IMA suggest the compounds potential as an anti-plasmodial candidate, warranting further biochemical validation of its mechanism of effect.

Keywords Iso-mukaadial acetate, Chloroquine, *Plasmodium falciparum*, RNA sequencing, Gene regulation, Cell adhesion, Glycolysis

Malaria is one of the oldest diseases known to humans, and historically, the fight against it relied heavily on plant-based remedies. Despite these longstanding efforts, it continues to pose a major global health burden, with *Plasmodium falciparum* responsible for most of the 263 million cases and 597,000 deaths reported in 2023[1]. The decreasing effectiveness of commonly used antimalarial drugs against *P. falciparum* has necessitated urgent efforts for the development of new drugs and vaccines that are more efficacious, safe, and affordable especially for developing countries[2]. The isolation of quinine from *Cinchona* bark and artemisinin from *Artemisia annua* represented key milestones in this fight[3]. *Warburgia salutaris*, a South African medicinal plant traditionally used for various ailments, has attracted interest among phytochemists and traditional healers[4,5] for its potential in managing malaria symptoms. Ethnobotanical research shows that decoctions from its leaves, bark, and roots have been used to treat fever, a hallmark symptom of malaria[4]. One of its bioactive constituents, iso-mukaadial

[1]Department of Biochemistry, Faculty of Science, University of Johannesburg, Johannesburg 2006, South Africa. [2]Pharmacology Division, Department of Pharmacy and Pharmacology, Faculty of Health Sciences, University of Witwatersrand, Johannesburg 2193, South Africa. [3]WITS Research Institute for Malaria (WRIM), Faculty of Health Sciences, University of Witwatersrand, Johannesburg 2193, South Africa. [4]Department Discipline of Biochemistry, School of Life Sciences, University of KwaZulu-Natal, Westville Campus, University Road, Westville 3629, South Africa. ✉email: msimelane@uj.ac.za

acetate (IMA), has demonstrated potent anti-plasmodial activity with IC_{50} of 1.43 µM[6], identifying IMA as a promising natural candidate for further development. IMA is a drimane sesquiterpenoid with an acetate functional group attached. It has been demonstrated to enhance glucose uptake[7], inhibit heat shock proteins 70 – 1 and 90[8,9], and induce apoptosis in cancer cells[10]. Similar phytochemical compounds such as warburganal, mukaadial and, muzigadialnextracted from *Warburgia stuhlmannii* Engl. root bark have demonstrated anti-plasmodial activity[11–13].

Advancing the research and development of antimalarial drugs requires a deeper understanding of the complex *P. falciparum* life cycle. Therefore, investigating the adaptation mechanisms of the parasite during its life cycle, particularly through the study of *Plasmodium* -produced proteins, could lead to the identification of novel drug targets[14]. These targets can be exploited for the development and design of antimalarial compounds that inhibit the progression and survival of the parasite[15]. Transcriptomic approaches can offer insight into the *Plasmodium* transcriptome, thus reflecting genome expression dynamics[16]. This, in turn, supports proteomics research focused on asexual malaria blood-stage profiling of expressed *Plasmodium* proteins, which regulates pathways and facilitates parasite development, maturity, pathogenesis, and transmission[17,18]. Transcriptional profiling using high-throughput ribonucleic acid (RNA) sequencing allows for a comprehensive analysis of RNA content at whole-genome transcription level. This method is instrumental in defining and quantifying RNA within cells or tissues under various developmental, physiological, and pathological conditions. This approach provides insights into gene structure, gene expression regulation, gene product function, and genome dynamics[19,20]. In this study, we applied RNA sequencing to compare the gene expression profiles during the intraerythrocytic stage following treatment with iso-mukaadial acetate (IMA) versus chloroquine (CQ) with the aim of identifying biological processes of differently regulated genes. The differential gene expression revealed insights into the molecular functions and pathways underlying IMA effect that can be used as starting point to determine IMA's potential molecular targets.CQ was included as a reference antimalarial to benchmark the transcriptional response of IMA-treated parasites.

Methods and materials

In vitro *Plasmodium falciparum* drug sensitivity assay and RNA extraction preparation

The chloroquine-sensitive *Plasmodium falciparum* NF54 strain was maintained in RPMI-1640 medium at 37 °C under a controlled atmosphere (5% CO_2, 3% O_2, 93% N_2)[21]. Cultures were synchronized to the ring stage using 5% (w/v) D-sorbitol. For drug sensitivity assays, synchronized cultures (2% parasitaemia, 2% haematocrit) were seeded into 96-well plates and treated with serial dilutions of Iso- mukaadial acetate (IMA) or chloroquine (CQ; positive control) starting at 10 µM. Drug-free cultures served as negative controls. After 48 h, plates were frozen at – 70 °C, thawed, and parasite growth was quantified via a parasite lactate dehydrogenase (pLDH) assay. pLDH activity was measured by adding 100 µL Malstat™ reagent and 20 µL of a nitroblue tetrazolium–phenazine ethosulfate (1:1) mixture, followed by incubation at 37 °C for 40 min. The reaction was stopped with 5% acetic acid, and absorbance was read at 620 nm. Growth inhibition curves and IC_{50} values were determined using GraphPad Prism® 5.0.0.

For RNA extraction, ~ 10 mL of synchronized ring-stage cultures (2% parasitaemia, 2% haematocrit) was treated with 10 µM IMA or CQ for 24 h. Untreated cultures were included as negative controls. After incubation, 1 mL aliquots were stored at – 80 °C until RNA extraction.

RNA extraction and library preparation

Total RNA was extracted from 1 mL *P. falciparum* cultures following Ponts et al. (2012)[22]. Cultures were thawed on ice, centrifuged (700 × g, 5 min), and pellets were lysed in prewarmed TRIzol® (37 °C; 5:1 ratio) for 5 min. Chloroform (1 mL) was added, and samples were centrifuged (12,000 × g, 4 °C, 30 min). The aqueous phase was transferred to a new tube, RNA was precipitated with 0.8 volumes ice-cold isopropanol, and pellets were collected by centrifugation (12,000 × g, 4 °C, 30 min), air-dried, and resuspended in 100 µL RNase-free DEPC-treated water. Samples were DNase-treated (11.3 µL 10× DNase I buffer, 2 µL DNase I, 30 min, on ice) and quantified using a NanoDrop ND-1000 spectrophotometer (2800–3200 ng/µL concentration recorded). RNA integrity was assessed via LabChip GX (PerkinElmer).

Human rRNA was removed using the MGIEasy rRNA depletion kit, and *Plasmodium* RNA libraries were prepared using the MGIEasy RNA Library Prep Set (10 ng–1 µg input) according to the manufacturer's protocol. Libraries were converted into single-stranded circular DNA and sequenced on an Illumina MiSeq platform at the Agricultural Research Council (South Africa).

Quality assessment and trimming of the sequencing reads

The raw RNA fastq files of all three conditions (IMA, CQ and drug-free) were evaluated for quality and adapter contamination via FastQC software[23]. Low-quality reads and adapter sequences were trimmed with Trimmomatic[24]. The processed reads were aligned to the *Plasmodium falciparum* 3D7 reference genome (GCF_000002765.5) from the National Center for Biotechnology Information (NCBI) using HISAT with default settings[25]. The HISAT output SAM files were sorted and converted to binary BAM files via SAMtools[26,27]. Gene-level counts were obtained from the processed BAM files via FeatureCounts software version 1.6.1[28] enabling the quantification of gene expression differences between CQ, IMA-treated and drug-free parasites. DESeq2 package in R[29] was used to identify differentially expressed genes (DEGs) using default parameters, which included controlling for fold change cutoffs, $\log_2$-fold-change shrinkage, and custom *P* values. Genes with a *P value*, adjusted for a false discovery rate (FDR) of < 0.05[30,31], and a $\log_2$-fold change ($\log_2$FC) of at least ± 1 between the studied groups were considered DEGs and retained for further analysis.

Differential gene expression analysis, gene enrichment, and pathway analysis

The enriched GO terms and pathways of DEGs were analyzed via gene set enrichment analysis (GSEA) tools such as ShinyGO (http://bioinformatics.sdstate.edu/go/), g: Profiler (https://biit.cs.ut.ee/gprofiler/convert), and PlasmoDB (https://plasmodb.org/plasmo/app/)[32–34]. Pathway biology and GSEA were performed to identify key biological processes and molecular functions associated with the differentially expressed genes in the IMA and CQ-treated parasites compared to drug-free parasites[35].

Ethical approval

This research has received ethical approval from the University of Johannesburg (reference: 2021-08-03/Salomane_Simelane), as well as from the University of the Witwatersrand Human Research Ethics Committee (M190579), Animal Ethics Committee (20190701-7O), and Institutional Biosafety Committee (20190404).

Results and discussions

In vitro anti-plasmodial activity of IMA and CQ

The in vitro intraerythrocytic stage of the chloroquine-sensitive (NF54) strain of *P. falciparum* exhibited concentration-dependent sensitivity to IMA and CQ. Previous reports indicated that IMA had an IC_{50} of 0.044 ± 0.10 µg/mL[6], which equates to 1.42 ± 0.32 µM when converted (µM = (µg/mL/MW)*1000). In this present study, IMA exhibited an IC_{50} value of 2.49 ± 0.49 µM and CQ had 0.013 µM, which was 190 times more potent than IMA ($P < 0.05$) as shown in Fig. 1 below.

According to the Medicines for Malaria Venture (MMV) guidelines, a potential anti-plasmodial compounds, whether derived from a plant extract or synthesized, is considered potent if it has an IC_{50} value of ≤ 1 µM and between 1 and 10 µM is considered highly active[36–38]. Therefore,, the observed IC_{50} of 2.49 µM regards IMA as an active compound with a promising anti-plasmodial activity. To determine how IMA exacts its Inhibitory activity, RNA Sequencing transcriptomics studies was used to identify the possible mode of inhibition.

Comparative analysis of DEGs induced by iso-mukaadial acetate treatment

The IMA-induced DEGs were visualized via enhanced volcano plots (Fig. 2). The most significantly down- and upregulated genes were identified based on the log_2 FC on the x-axis, which indicates the level of gene expression relative to normal expression levels. Table S1 shows top 50 IMA-induced down- and upregulated *Plasmodium* genes. The statistical significance of the expressed genes was determined based on the -Log_{10} FDR-associated *P value* for the down- and upregulated genes[39,40]. Differential expression analysis from normalizing gene-level counts using drug-free parasites resulted in 3047 IMA-induced DEGs, of which 2292 were downregulated, and 755 were upregulated compared with those in the CQ-induced group, which resulted in a total of 914 DEGs, with 462 upregulated and 452 downregulated genes as shown in Figure S1 and the corresponding Table S2.

The enhanced volcano plot in Fig. 2 shows that IMA-supplemented *Plasmodium* cells had more differently regulated genes that were expressed compared to CQ-supplemented cells as shown in Figure S1. To understand the most prevalent *Plasmodium* gene products for both CQ and IMA supplemented cells, a Venn diagram (Figure S6) of all the up and downregulated genes was generated to identify the most common regulated genes. The data was processed by removing all conserved genes with no known functions and the 18/28 S non-coding ribosomal RNA. Both CQ and IMA induced regulated genes were compared based on their Log_2 Fold Change values as outlined. A two-colour conditional formatting was used, with red representing downregulated genes and blue representing upregulated genes values, as shown in Table S3. A total of 603 common *Plasmodium* gene products were identified, with 445 gene product description annotated. Compared to CQ, IMA supplementation demonstrated a downregulation effect for most of the shared or common *Plasmodium* genes.

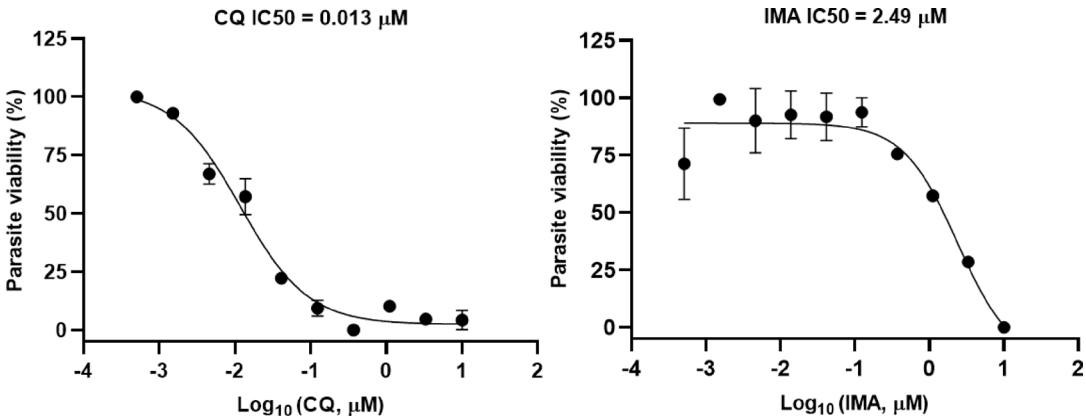


Fig. 1. Dose response analysis of CQ and IMA on asexual blood stage of *P. falciparum* NF54 done using *p*LDH assay. IC_{50} of CQ = 0.013 µM and IMA = 2.49 µM.

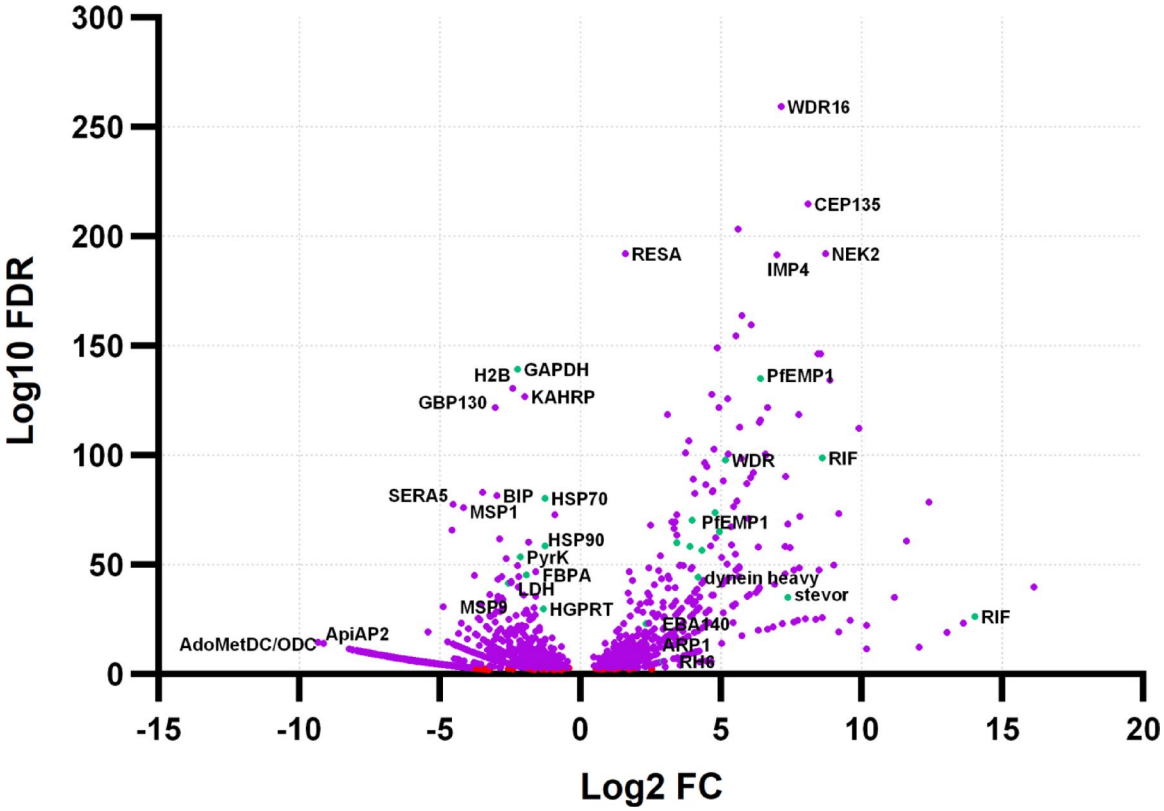


Fig. 2. An enhanced volcano plot of IMA-induced *P. falciparum* genes during the intraerythrocytic stage. Log_2FC represents the differentially expressed genes plotted against $-Log_{10}FDR$ denoting significant genes. An FDR of 0.001 was used to determine the genes with the greatest statistical significance. More significant *Plasmodium* genes were upregulated than downregulated.

The enriched down- and upregulated GO terms during the intraerythrocytic development stage

To interpret the biological significance of the down- and upregulated genes, key biological processes and molecular functions that occur during the intraerythrocytic development stage[41], GO enrichment analysis was conducted to evaluate the IMA-induced regulated genes compared with those of CQ. The enrichment analysis was performed using ShinyGO and calculations were done by comparing the baseline frequency of the complete set of annotated *Plasmodium* genes for a specific GO term in the *P. falciparum* 3D7 target species to the observed frequency of the IMA-induced regulated genes under the same GO term[32,42]. Further analysis for pathway IDs or GO terms was conducted using g: Profiler to identify *Plasmodium* proteins associated with the GO terms. PlasmoDB was also utilized to confirm the enrichment analysis of IMA- and CQ-induced regulated genes and to determine the corresponding gene product descriptions. GO molecular function was used to illustrate activities at the molecular level, carried out by the down- and upregulated genes, either as individual entities or as part of assembled complexes of *P. falciparum* gene products[43].

Plasmodium transcriptome induced by Iso-mukaadial acetate

The enrichment analysis of IMA-induced downregulated genes revealed significantly affected biological processes and molecular functions, as potential molecular MOA of IMA responsible for its anti-plasmodial effects via GSEA[44]. The transcriptomic changes induced by IMA, shown as downregulated and upregulated genes, are presented in an enhanced volcano plot (Fig. 2).

Analysis of upregulated *P. falciparum* genes induced by IMA

The top enriched GO terms for biological processes, ranked by fold enrichment (Fig. 3A), were primarily linked to symbiont adhesion (GO:0020035, GO:0044650, GO:0044406), modulation by symbionts (GO:0044003, GO:0044068, GO:0020013), and erythrocyte aggregation (GO:0034117, GO:0098609, GO:0020013). These processes—also observed with CQ treatment (Figure S2)—were largely driven by the RIFIN gene product ($Log_2FC = 8.5864$; $Log_{10}FDR = 98.8093$), STEVOR ($Log_2FC = 7.3640$; $Log_{10}FDR = 35.2440$), and *Pf*EMP1 ($Log_2FC = 6.4013$; $Log_{10}FDR = 135.1785$). In CQ-treated samples, the same gene products were also upregulated, with *Pf*EMP1 ($Log_2FC = 4.1843$; $Log_{10}FDR = 6.0852$), STEVOR ($Log_2FC = 4.9523$; $Log_{10}FDR = 3.2810$), and RIFIN ($Log_2FC = 5.9518$; $Log_{10}FDR = 10.8991$) showing notable fold changes.

The symbiont modulation interconnected biological network (Fig. 3B) was facilitated by *Pf*EMP1, STEVOR, and RIFIN, which are parasite-derived variant surface antigens involved in the cytoadherence of

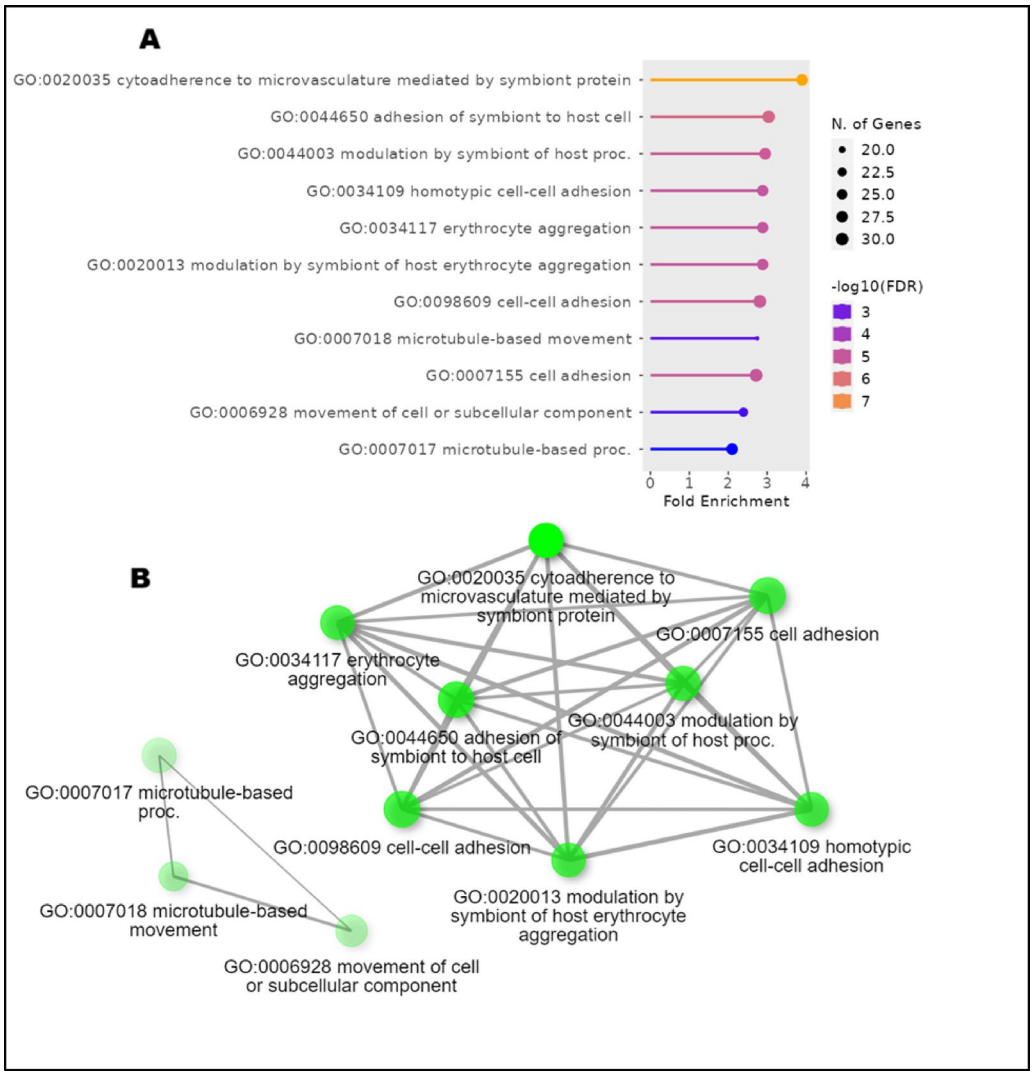


Fig. 3. Gene ontology biological processes of upregulated *Plasmodium* genes associated with IMA treatment. (**A**) The lollipop chart illustrates the cytoadherence to microvasculature mediated by *Plasmodium* proteins as the most enriched process and the most significantly involved biological process based on a higher Log_{10}FDR value. (**B**) An interconnected network diagram illustrating the connections between cell adhesion modulated by *Plasmodium* proteins. The size of the green nodes indicates more significantly enriched gene sets, whereas thicker edges represent a greater number of overlapping genes.

infected erythrocytes to healthy host erythrocytes[45,46]. These proteins have been observed to facilitate parasite sequestration and entry into erythrocytes, thus promoting parasite survival within the host[47]. The expression of *Pf*EMP1 has been associated with increased cytoadherence of infected erythrocytes to endothelial cells in different organs and immune system invasion by generating different antigens[46], allowing the parasite to remain in the host[45,48]. In a study involving pregnancy- associated malaria (PAM), the upregulation of a single var gene, *Pf*EMP1 was observed in *P. falciparum* parasite isolates after selection for adhesion to glycosaminoglycan chondroitin sulphate in vitro and PAM was linked to clonally variant surface antigen, which was the central process in the pathogenesis of *P. falciparum* infection[49]. As such, *Pf*EMP1 represents a therapeutic target, and understanding its MOA may lead to the development of strategies to hinder *Pf*EMP1-mediated cytoadherence to reduce the burden of infection[50]. Similarly, RIFIN and STEVOR proteins expressed on the surface of parasitized erythrocytes also contribute to enhanced immune system evasion, increased cytoadherence, and altered pathogenicity. As such, they are also possible targets for antimalarial drug development[45,51,52].

The interconnected symbiont adhesion shown in Fig. 3B was also mediated by a reticulocyte-binding protein ($Log_2FC = 2.9425$; $Log_{10}FDR = 5.763$) and an erythrocyte-binding antigen 140 ($Log_2FC = 2.3312$; $Log_{10}FDR = 23.0296$). Microtubule-based processes and the movement of cells or subcellular components were supported by several proteins, including actin-related protein 1 (ARP1; $Log_2FC = 2.3369$; $Log_{10}FDR = 13.6508$), centrosomal protein CEP135 ($Log_2FC = 8.0934$; $Log_{10}FDR = 214.8149$), WD repeat-containing protein ($Log_2FC = 5.1617$; $Log_{10}FDR = 97.8210$), dynactin subunit 2 ($Log_2FC = 5.3582$; $Log_{10}FDR = 67.4926$), and dynein heavy and light chains ($Log_2FC = 4.1839$; $Log_{10}FDR = 44.2857$; $Log_2FC = 5.9158$; $Log_{10}FDR = 87.1616$).

Molecular functions of upregulated genes induced by IMA

The upregulated GO terms related to molecular functions were ranked according to fold enrichment (Fig. 4A). These GO terms included microtubule motor activity, dynein intermediate chain binding, cell adhesion molecule binding, host cell surface and receptor binding, all of which are facilitated mostly by *P. falciparum* erythrocyte membrane protein 1 (*Pf*EMP1), virulence-associated protein 1 (VAP1), erythrocyte binding antigen-181 (EBA-181), reticulocyte binding protein homolog 5 & 4 (Rh5 & Rh4) and Duffy binding-like (DBL) merozoite surface proteins. The most significant IMA-induced upregulated molecular functional activities are cell adhesion molecule binding and host cell surface (Fig. 4B). Compared with those induced by CQ (Figure S3), the enriched molecular function GO terms included host cell surface binding, cyclic compound binding, nucleoside binding, protein dimerization activity and structural molecule activity. Host cell surface binding is facilitated by GPI-anchored micronemal antigen, apical membrane antigen 1 (AMA1), circumsporozoite (CS) protein, cytoadherence-linked asexual protein 3.1 (CLAG3.1), erythrocyte binding antigen-140 (EBA-140), *Pf*EMP1, merozoite TRAP-like protein, merozoite surface protein, and reticulocyte binding protein 2 homolog a.

These proteins facilitate parasite sequestration and entry into erythrocytes, promoting parasite survival within the host[47]. The upregulation of VAP1, EBA-181, and Rh5 & Rh4 proteins has been associated with virulence and binding mechanism of *Plasmodium* species[53]. The upregulation of VAP1 promotes adhesion to host endothelial

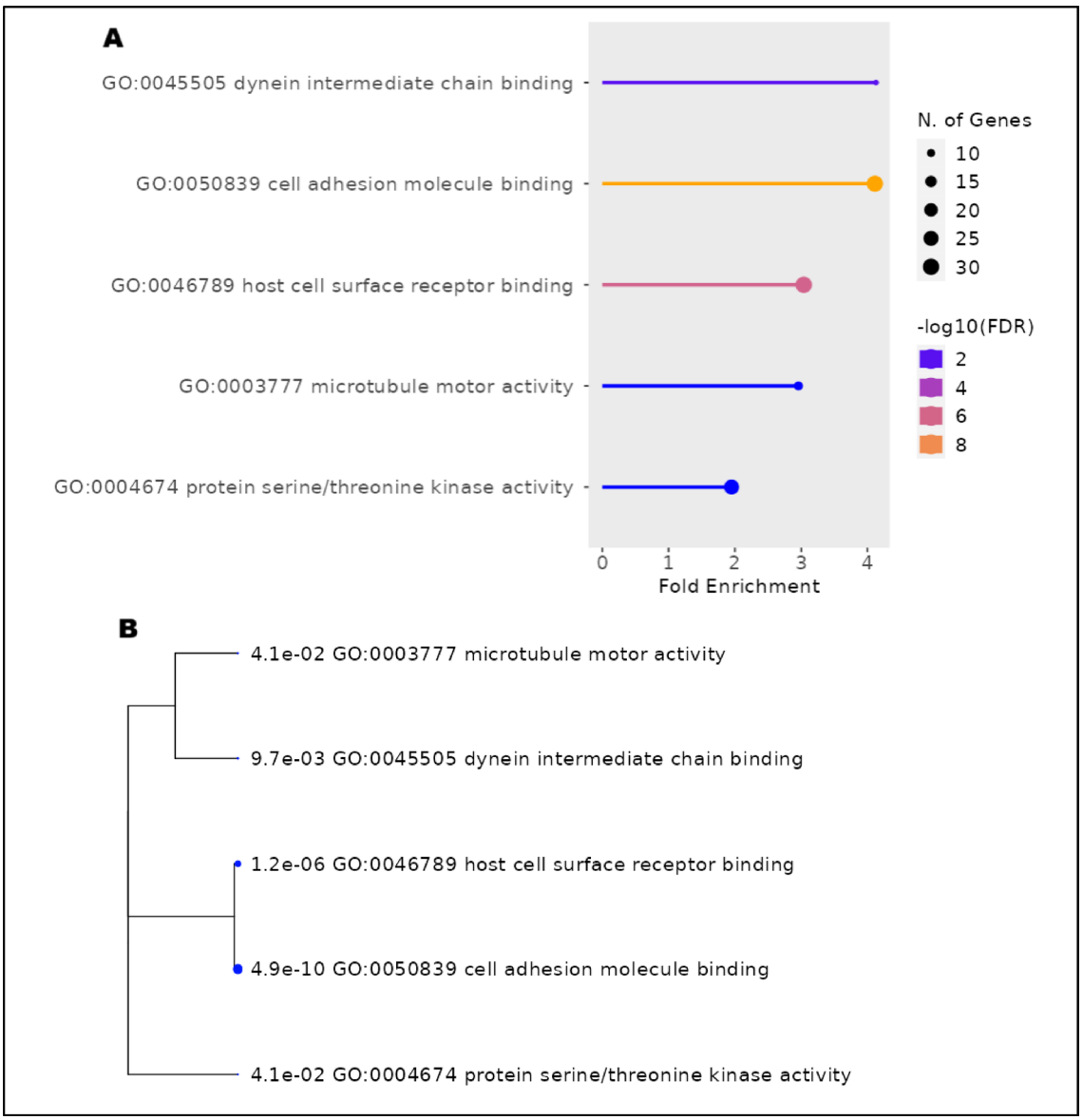


Fig. 4. Gene ontology for the molecular functions of IMA-induced upregulated genes. (**A**) Lollipop chart showing that cell adhesion binding activity was the most enriched and the most significant molecular function, with a log10FDR > 8. (**B**) A hierarchical clustering tree summarizing the correlations among the significant molecular functional activities, with pathways sharing genes clustered together. Larger blue dots indicate more significant FDR values.

cells in various tissues, preventing clearance of erythrocytes infected by the spleen. EBA-181 is upregulated for merozoite invasion into erythrocytes, and Rh5 and Rh4 form part of the reticulocyte-binding protein homologs important for invasion mechanism of merozoites[54]. The expression of these virulent genes/proteins mediate *Plasmodium* invasion into erythrocytes during the intraerythrocytic development stage. The incorporation of small inhibitor molecules that target these virulent genes in combination with IMA could hypothetically reduce *Plasmodium* invasion.

Analysis of downregulated *P. falciparum* genes induced by IMA

The top 20 downregulated GO terms for biological processes were ranked based on fold enrichment (Fig. 5A). The most significantly downregulated biological processes involved peptidyl-proline modification (GO:0018208) and peptidyl-prolyl isomerization (GO:0000413), both of which are catalyzed by peptidyl-prolyl cis-*trans* isomerase (PPIase), with a Log_2FC of −5.6296 and a $Log_{10}FDR$ of 5.7352. PPIases are responsible for controlling *Plasmodium* proteins folding by catalyzing the isomerization of peptide bonds at proline residues[55], and their downregulation could lead to accumulation of misfolded *Plasmodium* proteins, causing stress to the cellular machinery[56,57]. The glycolytic process (GO:0006096) and carbohydrate catabolic process (GO:0016052) linked to ATP generation from ADP and ADP metabolic processes were also downregulated[58,59]. Key enzymes affected included L-lactate dehydrogenase, (Log_2FC = −2.5694; $Log_{10}FDR$ of 41.5215); enolase (Log_2FC = −2.2364; $Log_{10}FDR$ = 49.6179); fructose-bisphosphate aldolase, (Log_2FC = −1.9181; $Log_{10}FDR$ = 45.4065); GAPDH (Log_2FC = −2.2332; $Log_{10}FDR$ = 139.4728); pyruvate kinase (Log_2FC = −2.1387; and $Log_{10}FDR$ = 53.5869). The most significant biological processes with CQ dosing are DNA replication processes (Figure S4A), which are potentially impacted by DNA synthesis disruption due to downregulated of glycolic and redox enzymes[60].

Plasmodium parasites rely on glycolysis as the primary source of energy, especially during the intraerythrocytic stages[61], the downregulation of enolase limits the formation of phosphoenolpyruvate, which is an important key step in ATP production and is required for essential parasitic cellular functions[62]. The downregulated expression of GAPDH halts the glycolytic pathway, limiting glucose metabolism and leading to reduced ATP generation[63,64]. Therefore, reduced ATP production *Plasmodium* during the intraerythrocytic development stage[65,66] due to IMA exposure resulted in suppression of *Plasmodium* metabolic pathways, as indicated by the downregulation of these glycolytic enzymes, causing disturbances in parasitic energy metabolism, protein homeostasis, and general survival.

The DNA replication processes (GO:0006268, 0065004) shown in Fig. 5B and Figure S4B were also affected, with significant downregulation of key proteins, including the DNA mismatch repair protein MSH6 (Log_2FC −6.3356; $Log_{10}FDR$ 7.10859), DNA repair protein RAD51 (Log_2FC −4.8835; $Log_{10}FDR$ 4.4462), DNA replication licensing factor MCM3 (Log_2FC −2.1358; $Log_{10}FDR$ 15.0226), DNA topoisomerase 3 (Log_2FC −4.7543; $Log_{10}FDR$ 4.2404), GINS subunit Psf3 (Log_2FC −4.2178; $Log_{10}FDR$ 3.4372), and replication protein A1 (Log_2FC −6.1249; $Log_{10}FDR$ 6.6831). IMA exposure likely induced DNA damage through oxidative stress, compromising genomic integrity during the intraerythrocytic stage[67]. This was exacerbated by reduced expression of DNA repair proteins such as RAD51 and topoisomerase 3, which are essential for maintaining replication and repair machinery[68,69]. Downregulation of the licensing factor MCM3 further disrupted replication initiation, limiting DNA synthesis and cell division[70]. The parasite's capacity to divide and multiply during the intraerythrocytic stage could have been hampered by IMA-induced disruption, leading to imperfect or partial DNA replication[70].

Additionally, replication fork stalling and increased parasite mortality may have resulted from difficulties with DNA unwinding caused by downregulated DNA topoisomerase 3, which also hinders transcription and replication[71,72]. Replication stress and inadequate DNA synthesis can occur by downregulating the GINS complex subunit Psf3, which compromises replication fork stability and hinders the ability of the parasite to replicate its genome[73,74]. As a major eukaryotic ssDNA-binding protein, reduced replication protein A1 (RPA1) expression can cause single-stranded DNA to become unstable, increasing the possibility of DNA damage and hindering repair[75]. Collectively, the downregulation of these proteins could have halted the cell cycle, collapsed the replication fork, and decreased parasite survival in the IMA-treated parasites. The potential of DNA replication machinery being affected by CQ was also observed with the downregulation of DNA replication and repair proteins, suggesting a disruption in the parasite's ability to maintain its genome integrity[76]. The lowered expression of DNA helicase could have impeded the progression of the replication fork, causing slower DNA replication and leading to cell cycle arrest and reduced cell proliferation[77]. The downregulation of the DNA replication licensing factor MCM3, which could have interfered with the replication licensing process, is important for preparing DNA for replication. This disruption results in incomplete or faulty DNA replication, therefore hindering the parasite's ability to divide and proliferate during the intraerythrocytic development stage[70].

Molecular functions of downregulated genes included by IMA

The GO molecular functions of the IMA-induced downregulated genes included but were not limited to folding chaperones, peptidase activity, ubiquitin binding, phosphatase activity, DNA binding and replication, as shown in Fig. 6 compared to Figure S5 for CQ supplementation. These molecular functions were sorted according to fold enrichment. GO term analysis revealed the activities of these folding chaperones are facilitated by heat shock proteins (Hsps 90, 110, 70, and 60), a T-complex protein 1 subunit, chaperonins and the DNAJ protein[78,79]. Phosphoprotein phosphatase activity is carried out by a group of phosphatases, including serine/threonine protein phosphatases, protein phosphatases PPM 5–7, and protein tyrosine phosphatases[80,81].

A reduction in HSP60 expression can disrupt mitochondrial function, which is crucial for energy production and parasite development[82]. The T-complex protein 1 subunit forms part of the chaperonin complex (CCT), which assists in the folding of actin and tubulin, which are essential cytoskeletal components, and the downregulation of this chaperonin complex can cause improper folding of *P. falciparum* actin and tubulin, resulting in a more

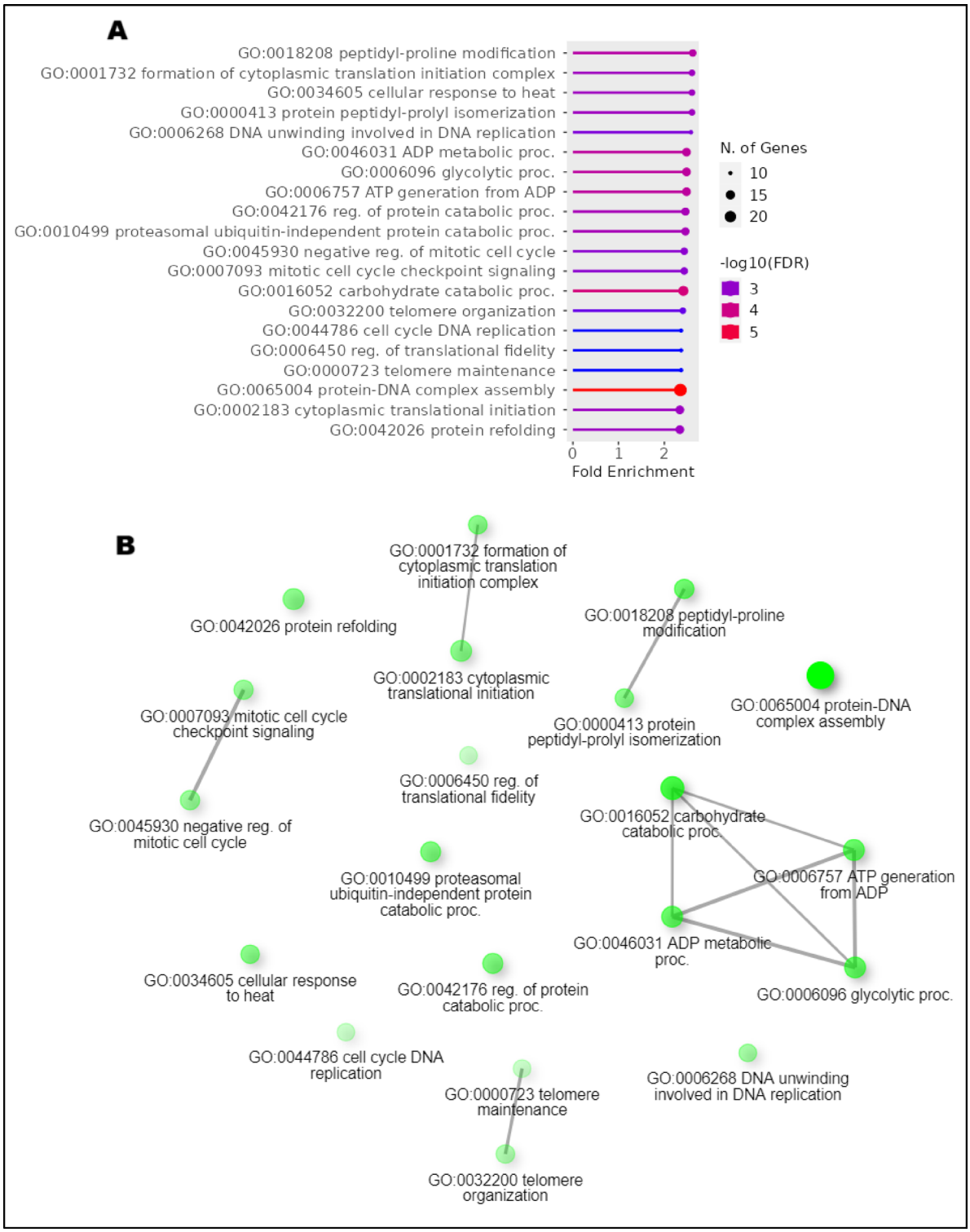


Fig. 5. Gene Ontology analysis of biological processes associated with downregulated Plasmodium genes in response to IMA treatment. (A) The lollipop chart illustrates the peptidyl-proline/prolyl modification process as the most enriched process and the DNA–protein complex process as the most significantly involved biological process based on a higher Log10FDR value. (B) An interconnected network illustrating the connections between the generated biological processes. The size of the green nodes indicates more significantly enriched gene sets, whereas thicker edges represent a greater number of overlapping genes.

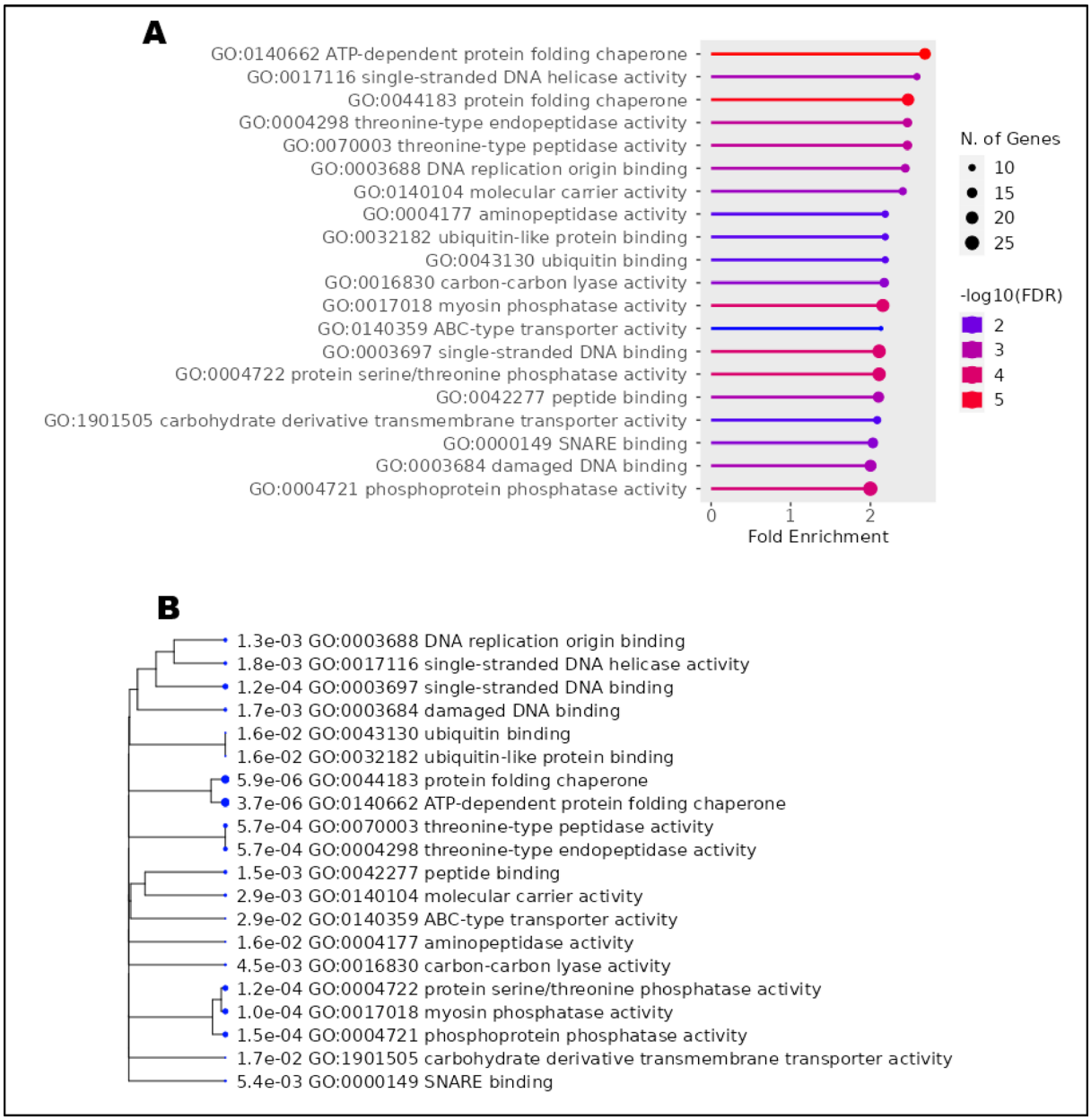


Fig. 6. Gene ontology for the molecular functions of IMA-induced downregulated genes. (**A**) The lollipop chart illustrates the protein folding chaperone as the most enriched and the most significant molecular function with a higher -Log_{10}FDR > 5. (**B**) A hierarchical clustering tree summarizing the correlations among the significant molecular functional activities, with pathways sharing genes clustered together. Larger blue dots indicate more significant FDR values.

defective cell membrane and cellular movement[78,83]. Downregulated phosphatase activity can disrupt cellular signaling, impair cell cycle regulation, and alter stress response mechanisms[81]. This decreased expression may have weakened the parasite's ability to manage stress and compromised critical signaling pathways needed for cell proliferation and invasion, thus reducing the parasite's adaptability when dosed with IMA.

The stress response, stability, and protein folding of *Plasmodium* when exposed to IMA may depend on heat shock proteins (HSPs). The downregulation of several HSPs and other chaperone-related proteins might have potentially impair critical cellular functions such as DNA replication and the ability to maintain protein homeostasis during stress[84].

Transcriptional network interactions of IMA regulated genes

According to the network interactions between the down- and upregulated genes that were determined when supplemented with IMA, heat shock protein 70 (Hsp70) (*PF*3D7_0831700) seems to have formed the most interactions with other *Plasmodium* proteins, as demonstrated in Fig. 7.

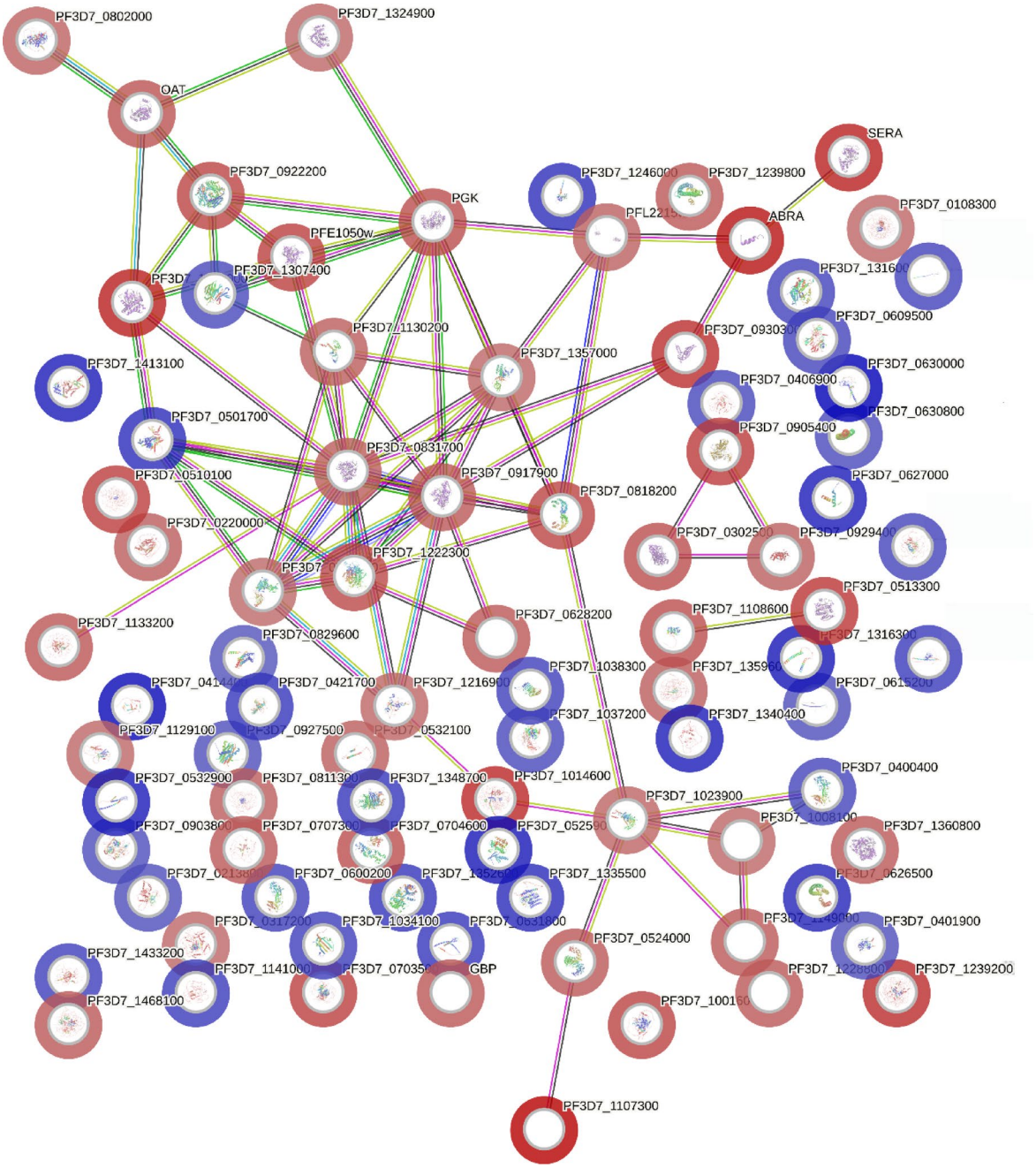


Fig. 7. Protein–protein interaction network of *Plasmodium* proteins when the parasite was supplemented with iso-mukaadial acetate (IMA). The interactions were determined via String (https://string-db.org/), which uses Log_2FC to denote the downregulated (red) and upregulated (blue) genes.

Hsp70 is a molecular chaperone that is expressed in response to stress. It has various functions, such as facilitating the folding of recently produced proteins, facilitating the movement of proteins and vesicles within cells, facilitating the assembly and disassembly of complexes, and breaking down proteins that are no longer needed[85,86].

Consequently, this chaperone extensively regulates protein balance by overseeing both the quality control and disposal of proteins under typical and stressful circumstances[87,88]. Another Hsp70 (*PF*3D7_0917900) was determined to be the main intermediate connector. Both of these Hsp70s interact with downregulated phosphoglycerate kinase (PGK) (*PF*3D7_09225000) and elongation factor 1-alpha (*PF*3D7_1357000), which enhances the GTP-dependent attachment of aminoacyl-tRNA to the A-site of ribosomes in the course of protein synthesis[89]. The current work adds to our previous claims, demonstrating IMA as an inhibitor of the chaperone activity of *P. falciparum* essential proteins such as Hsp70[9] and Hsp90[8]. The Inhibition of these chaperones disrupts the parasite's ability to maintain protein quality control and proper folding, ultimately impairing its survival under both normal and stress-induced conditions. Moreover, the observed interactions with proteins involved

in metabolism and translation suggest that the inhibitory effects of IMA may extend beyond chaperone function, either through direct interaction or by network interruption mechanism, and thus potentially affecting multiple targets within the parasite's biology. Nonetheless, additional studies are still required to confirm the inhibitory role of IMA *on P. falciparum*. Taken together, these results highlight the multifaceted role of Hsp70s in parasite viability and underscore the potential of IMA as a promising candidate for antimalarial drug development. Targeting chaperone-mediated pathways may therefore represent an effective strategy for disrupting essential cellular functions in *P. falciparum*, offering new avenues for therapeutic intervention. Future studies investigating the broader network of protein interactions and the stage-specific effects of IMA inhibition will be valuable in fully elucidating its mechanism of action and therapeutic potential.

Most of the network interactions are observed with the downregulated genes compared with the upregulated genes, forming only three interactions. The upregulated anaphase-promoting complex subunit 3 (*PF*3D7_0501700; Log_2FC 7.7654) is also interconnected with the abovementioned Hsp70s. *P. falciparum* erythrocyte membrane protein 1 (*Pf*EMP1) (*PF*3D7_0400400) was associated with downregulated genes encoding zinc finger protein (*PF*3D7_1008100) and chromodomain-helicase-DNA-binding protein 1 (*PF*3D7_1023900).

Analysis of IMA and CQ similar expressed genes

The 603 commonly expressed genes (Figure S8) shown in Table S3 demonstrated both IMA and CQ mechanisms of action based on the drug-induced stress response and compensatory mechanisms. CQ's mechanism of action has been previously determined to involve inhibiting heme polymerase and preventing heme detoxification into hemozoin[90]. Heme accumulation was suggested to inhibit glyceraldehyde 3-phosphate dehydrogenase (GAPDH) and thioredoxin reductase (TrxR), thus disrupting mechanism for DNA synthesis[60]. In our study, GAPDH deregulation Log2 FC value was observed at 0.5435 and − 2.2332 for CQ and IMA, respectively. These values theoretically suggest that parasite death by CQ was not through GAPDH inhibition. However, for IMA this is possible mode of inhibition affecting glycolysis. The thioredoxin systems are important for redox regulation, protection against oxidative stress. TrxR and Thioredoxins (Trx) play crucial roles in maintaining the parasite's redox balance and enabling its survival within the host cell[91]. Thioredoxin (Trx) 1, which is reduced by TrxR back to their active form[92] was observed at Log2FC 0.6014 and − 6.8967 with CQ and IMA. Trx 2 isoform was downregulated by CQ with Log2 FC of −4.1278. While with IMA drug exposure Trx 3 was upregulated and TrxR downregulated with Log2 FC 2.9378 and − 6.1547; respectively. The downregulation of the parasite thioredoxin systems supposedly lead to the increased vulnerability to oxidative stress causing impaired protein regulation and eventually parasite death[92,93].

Furthermore, chloroquine resistance has been attributed to the *P. falciparum* chloroquine resistance transporter (*Pf*CRT), a member of the ATP-binding cassette (ABC) transporter protein family[94,95].ABC4 and ABC5 exhibited a fold expression of Log2FC −6.2547 at Log10FDR 5.2409 and − 4.7324 at Log10FDR 2.9203, respectively in our study. The downregulation of these ABC transporter proteins is linked to impaired efflux of CQ's from the digestive vacuole, facilitating continued haemoglobin degradation inhibition of parasite proteases for nutrient salvaging and maintaining the colloid-osmotic balance of the infected erythrocyte[96]. Different gene id's denoting erythrocyte membrane protein 1 (*Pf*EMP1) were observed to be upregulated up until Log2FC of 5 with both CQ and IMA. Therefore, hypothetically the resulted anti-plasmodial activity of IMA was not through *Pf*EMP1 when compared to CQ.

IMA -induced Kyoto encyclopedia of genes and genomes pathway analysis

KEGG pathway analysis[97–99] revealed biological processes that were strongly impacted by IMA downregulated genes. Gaining insight into these downregulated pathways can aid in understanding how IMA impacts parasite signaling, metabolism, or other biological functions. The KEGG pathways that were significantly downregulated were the pentose phosphate pathway, DNA replication pathway and glycolysis/gluconeogenesis pathway, which were of particular interest, as we investigated the effects of IMA on these pathways. The Enzyme Commission (EC) numbers were used to denote each identified gene or enzyme found in the abovementioned pathways[100].

Glycolysis/gluconeogenesis KEGG pathway analysis

The glycolytic process and carbohydrate catabolic process linked to ATP generation from ADP and ADP metabolic processes[58] were among the most downregulated GO terms related to essential *P. falciparum* biological processes following IMA treatment[101]. Understanding how the decreased expression of glycolytic proteins affects the survival of *P. falciparum* is paramount for the development and design of IMA as a potential antimalarial agent. The downregulated glycolysis/gluconeogenesis enzymes (Figure S7[102] included phosphoglucomutase (5.4.2.2), hexokinase (2.7.1.1), glucose-6-phosphate isomerase (5.3.1.9), 6-phosphofructokinase (2.7.1.11), fructose-bisphosphate aldolase (4.1.2.13), triose-phosphate isomerase (5.3.1.1), glyceraldehyde-3-phosphate dehydrogenase (1.2.1.12), phosphoglycerate kinase (2.7.2.3), phosphoglycerate mutase (5.4.2.11), phosphoenolpyruvate carboxykinase (4.1.1.49), pyruvate kinase (2.7.1.40), acetate-CoA ligase (6.2.1.1), and dihydrolipoyl dehydrogenase (1.8.1.4)[103]. The number of ECs of these enzymes is highlighted in red to indicate and emphasize where they are found in the glycolytic pathway and which downstream enzymatic reactions they influence.

Since glycolysis is crucial for ATP production in *P. falciparum*, which thrive in low-oxygen environments and relies on glycolysis for energy[104], the downregulation of core glycolytic enzymes such as hexokinase, 6-phosphofructokinase, aldolase, and pyruvate kinase suggests that the primary pathway for glucose metabolism is likely impaired[105,106]. The inhibition of these enzymes could therefore decrease ATP generation, deprive the parasite of energy and increase parasite death. The current study further supports the recent findings of Zuma and colleagues (2025), who demonstrated a protein-ligand binding interaction between IMA and *P. falciparum* hexokinase. Through both computational and in vitro approaches, IMA was shown to bind directly to hexokinase

with measurable affinity. This interaction highlights the potential for developing novel antimalarial drugs that specifically target this mechanism, highlighting hexokinase as an important target molecule[107]. Glyceraldehyde-3-phosphate dehydrogenase and triose phosphate catalyze key steps in glycolysis, turning triose phosphates into pyruvate[63,108]. Therefore, the decreased expression of these proteins further impedes the production of ATP and NADH, upsetting the cellular redox balance and reducing energy output. Two enzymes involved in gluconeogenesis and acetyl-CoA synthesis are phosphoenolpyruvate carboxykinase (PEPCK)[109] and acetate-CoA ligase. Downregulation of the latter enzymes implies decreased acetate conversion to acetyl-CoA and a compromised ability to produce glucose from noncarbohydrate precursors. The decreased amounts of acetyl-CoA may restrict biosynthesis pathways, impacting the production of lipids and other macromolecules necessary for parasite survival[110].

Therefore, targeting these enzymes may be a promising approach for antimalarial treatments[58,111]. By fully understanding these downregulated enzymes, important metabolic checkpoints can be identified and potentially used to further optimize the inhibition of vital *P. falciparum* energy and biosynthesis pathways by IMA. Furthermore, to convert glucose into pyruvate for energy production, the glycolytic route requires the enzymes 6-phosphofructokinase (2.7.1.11), glucose-6-phosphate isomerase (5.3.1.9), and fructose-bisphosphate aldolase (4.1.2.13)[112]. Given that *P. falciparum* thrives in an environment with limited energy, the downregulation of these enzymes via the glycolytic route implies a decrease in glycolytic flow, which decreases ATP generation.

Pentose phosphate pathway KEGG analysis

Adjacent to the glycolysis/gluconeogenesis pathway is the interconnected pentose phosphate pathway (PPP) (Figure S8[102], which performs several tasks involving the parasite's high requirement for nucleotides, reducing power, and carbon intermediates for several metabolic processes[113]. Both ribulose-phosphate 3-epimerase (5.1.3.1) and glucose-6-phosphate dehydrogenase (G6PD)–6-phosphogluconolactonase (1.1.1.49) are involved in the oxidative and nonoxidative stages of the PPP, respectively. The PPP supplies *P. falciparum* ribose-5-phosphate for nucleotide synthesis and NADPH for redox equilibrium[114]. In this case, the downregulation of both enzymes implies that *P. falciparum* would be less able to synthesize nucleotides for DNA replication and repair and manage oxidative stress (due to less NADPH) caused by IMA. Additionally, a crucial enzyme in the nonoxidative PPP is transketolase (2.2.1.1), which is connected to glycolysis by transforming sugars such as ribose-5-phosphate into glyceraldehyde-3-phosphate[115]. The decreased expression of transketolase might make it more difficult for the parasite to strike a balance between the synthesis of amino acids and nucleotides and energy generation[116]. For the synthesis of the sugar backbone of nucleotides, deoxyribose-phosphate aldolase (4.1.2.4) and ribose-phosphate pyrophosphokinase (PRPP synthetase; 2.7.6.1) are essential. For example, the production of phosphoribosyl pyrophosphate (PRPP), a precursor in nucleotide synthesis, requires PRPP synthetase[117]. When these enzymes are downregulated, nucleotide availability is drastically reduced, impairing the parasite's capacity to synthesize and repair DNA[117,118].

The downregulation of the PPP and glycolytic enzymes indicated a weakened antioxidant defense mechanism (due to less NADPH) and decreased energy production, increasing the vulnerability of the parasite to oxidative harm caused by the presence of IMA within the parasite[119,120]. *P. falciparum* may also have trouble maintaining adequate nucleotide pools, which could impair its ability to replicate, repair, and transcribe DNA[121]. This is indicated by the downregulated expression of enzymes necessary for nucleotide biosynthesis, such as ribose-phosphate pyrophosphokinase and PRPP synthetase. Given *P. falciparum*'s reliance on the glycolysis and PPP pathways for energy and survival, further suppression of these downregulated enzymes may increase the parasite's metabolic stress, resulting in parasite death[122]. Because IMA takes advantage of nucleotide synthesis vulnerability, the parasite cannot successfully replicate and repair its DNA, which eventually limits its capacity for survival and replication.

DNA replication KEGG pathway analysis

IMA-induced DNA damage may be indirectly due to oxidative stress affecting the genomic integrity of intra-erythrocytic parasites. This is perpetuated by the downregulation of DNA topoisomerases α-primase and ε-complex, which are important for the DNA replication and repair machinery required to overcome IMA-induced damage[68,69]. However, their lower expression indicates impaired DNA repair machinery, resulting in decreased *Plasmodium* DNA replication and potentially affecting parasite survival and proliferation. Replication licensing is essential for obtaining *P. falciparum* DNA ready for replication, and it is disrupted when the DNA replication licensing component MCM complex is downregulated as shown in Fig. 8 below[123]. The capacity of intraerythrocytic parasites to divide and multiply may be hampered by this disruption, leading to imperfect or partial DNA replication[70].

Additionally, replication fork stalling and increased parasite mortality may result from problems with DNA unwinding caused by downregulated DNA topoisomerase complexes that hinder transcription and replication. Reduced replication protein A1 (RPA1) expression causes single-stranded DNA to become unstable, increasing the possibility of DNA damage and hindering repair. As a result of IMA treatment, downregulation of this protein could have halted the cell cycle, caused replication fork collapse, and decreased parasite survival.

The ability of *P. falciparum* to replicate and repair its DNA may be significantly impacted by the downregulation of replication factor C subunit 1 (RFC1) and *P. falciparum* proliferating cell nuclear antigen (PCNA), which may limit the ability of the parasite to multiply within host cells[124,125]. Reduced PCNA expression results in delayed or insufficient replication by lowering the efficiency of DNA synthesis. Since fewer repair proteins are available to fix any errors or damage, this can slow the replication fork and increase DNA damage[126]. Furthermore, the decreased expression of RFC1 can prevent DNA synthesis from starting because it interferes with the assembly

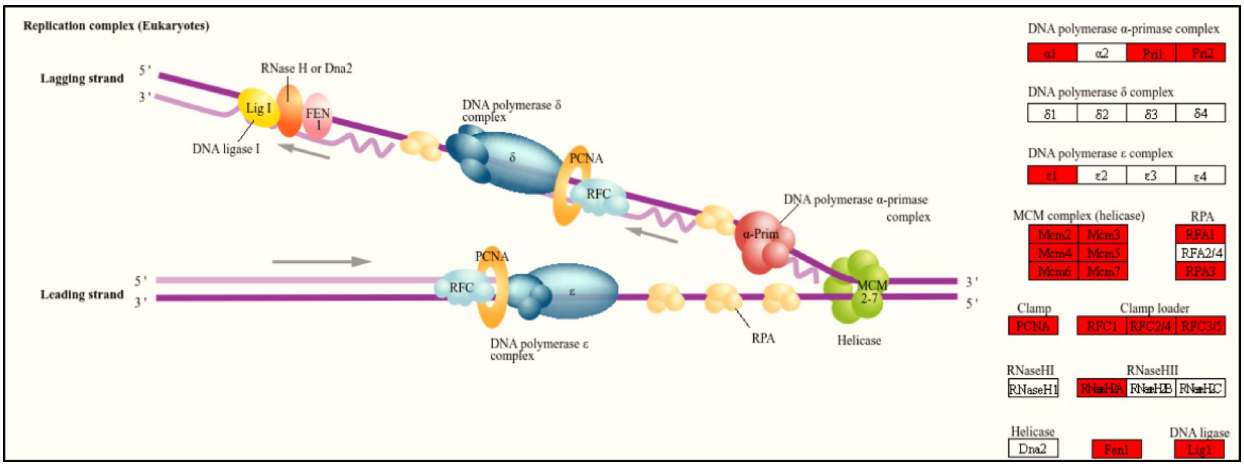


Fig. 8. The DNA replication KEGG pathway (*Pf*a03030)[98,123] in intraerythrocytic *P. falciparum* parasites treated with IMA. The downregulated enzymes are represented with numbers and highlighted in red.

of the RFC complex and the ability of PCNA to load onto DNA. This could hinder genome duplication, lower rates of proliferation, and possibly initiate reactions that damage DNA[127].

Since *P. falciparum* behaves as an auxotroph, relying on *de novo* pathways for pyrimidine nucleotide biosynthesis and the purine salvage pathway for synthesizing cofactors and nucleic acids essential for merozoite formation[128]. Hypoxanthine-Xanthine Phosphoribosyl transferase (HGPRT), a purine salvage enzyme responsible for reversibly transferring phosphoribosyl moiety of phosphoribosyl pyrophosphate (PRPP) to the nucleobase 6-oxopurines to produce monophosphorylated nucleotides required for nucleic acids synthesis[129] was differentially downregulated at Log2FC −1.3128 by IMA dosing. This could have impeded parasite's nucleic acid synthesis, crucial for its growth and DNA replication during the asexual intraerythrocytic stage[130]. The binding affinity of IMA to HGPRT was demonstrated by molecular dynamics simulations, ultra-violet (UV) visible spectrometer analysis and microscale thermophoresis studies[131]. The binding affinity studies had supported the previously observed in vitro antimalarial results and IMA – HGPRT complex.

While in vitro validation studies are increasingly becoming standard in transcriptomic research, practical constraints such as limited resources can sometimes hinder their application. Nevertheless, in this document, we present data that corroborate our earlier findings, confirming that IMA acts as an inhibitor of the chaperone activity of key Plasmodium proteins, including Hsp70[9] and Hsp90[8]. Additionally, our recent work has demonstrated the binding affinity of IMA to hexokinase[107], further supporting its modulatory role in glycolytic enzymes. Collectively, these results strengthen the evidence for IMA as a multifaceted inhibitor, with the potential to target multiple essential proteins in *P. falciparum*. These findings not only enhance our understanding of IMA's mechanism of action but also underscore its potential as a promising candidate for antimalarial drug development.

Conclusion

IMA and CQ were observed to hinder *Plasmodium* survival by suppressing key proteins, including DNA polymerase and the DNA replication licensing component MCM complex, that are essential for DNA synthesis and repair during the intraerythrocytic cycle. IMA theoretically disrupted parasite metabolism by inhibiting critical enzymes in glycolysis and the pentose phosphate pathway, leading to the reduced ATP and NADPH production, energy depletion, and increased oxidative stress. Even though both IMA and CQ upregulated adhesion-associated gene families (*Pf*EMP1) to increase cytoadherence of infected erythrocytes to endothelial cells in different organs, allowing the parasite to remain in the host and enhancing immune system invasion. The combined effects on DNA replication, energy metabolism, and redox homeostasis limited the parasite's ability to adapt within host cells during drug exposure. KEGG pathway analysis of the downregulated genes highlighted potential IMA targets, including glyceraldehyde-3-phosphate dehydrogenase, DNA replication proteins, and pentose phosphate pathway enzymes. One of the limitations of our study is the insufficient number of biological replicates, which may impact the robustness and generalizability of our findings. In the second phase of this study, we aim to include a greater number of replicates to strengthen the reliability of our results. Additionally, investigating stage-specific inhibition using transcriptomic assays would provide higher-resolution insights into the molecular effects and better elucidate the mechanisms resulting from IMA treatment.

Data availability

The RNA sequencing data generated in this study is available under NCBI BioProject accession number PRJNA1240819 with the title: RNA Sequencing of *P. falciparum* treated with IMA. Accessible link: (https://www.ncbi.nlm.nih.gov/bioproject/?term=PRJNA1240819).

Received: 20 June 2025; Accepted: 28 October 2025

Published online: 27 November 2025

References

1. Venkatesan, P. WHO world malaria report 2024. *Lancet Microbe* **2025**, 101073. https://doi.org/10.1016/j.lanmic.2025.101073 (2025).
2. Rathmes, G. et al. Global Estimation of anti-malarial drug effectiveness for the treatment of uncomplicated plasmodium falciparum malaria 1991–2019. *Malar. J.* **19**, 374. https://doi.org/10.1186/s12936-020-03446-8 (2020).
3. Guchait, A., Kumar, A., Singh, R., Joshi, G. & Dwivedi, A. R. A review on reported phytochemicals as druggable leads with antimalarial potential. *Med. Chem. Res.* **32**, 1633–1657. https://doi.org/10.1007/s00044-023-03113-y (2023).
4. Maroyi, A. The genus warburgia: A review of its traditional uses and Pharmacology. *Pharm. Biol.* **52** (3), 378–391. https://doi.org/10.3109/13880209.2013.837935 (2014).
5. Senkoro, A. M. et al. The genetic legacy of fragmentation and overexploitation in the threatened medicinal African pepper-bark tree, Warburgia salutaris. *Sci. Rep.* **10** (1), 19725. https://doi.org/10.1038/s41598-020-76654-6 (2020).
6. Nyaba, Z. N. et al. Isolation, characterization, and biological evaluation of a potent anti-malarial Drimane sesquiterpene from Warburgia salutaris stem bark. *Malar. J.* **17** (1), 296. https://doi.org/10.1186/s12936-018-2439-6 (2018).
7. Msomi, N. Z., Shode, F. O., Pooe, O. J., Mazibuko-Mbeje, S. & Simelane, M. B. C. Iso-mukaadial acetate from Warburgia salutaris enhances glucose uptake in the l6 rat myoblast cell line. *Biomolecules* **9** (10), 520. https://doi.org/10.3390/biom9100520 (2019).
8. Nndwammbi, A. A. T. et al. Ursolic acid acetate and iso-mukaadial acetate bind to plasmodium falciparum Hsp90, abrogating its chaperone function in vitro. *Naunyn Schmiedebergs Arch. Pharmacol.* **397** (7), 5179–5192. https://doi.org/10.1007/s00210-024-02944-9 (2024).
9. Salomane, N., Pooe, O. J. & Simelane, M. Iso-mukaadial acetate and ursolic acid acetate inhibit the chaperone activity of plasmodium falciparum heat shock protein 70-1. *Cell. Stress Chaperones*. **26** (4), 685–692. https://doi.org/10.1007/s12192-021-01212-6 (2021).
10. Raphela-Choma, P. P., Lukhwareni, R., Simelane, M. B. C., Motadi, L. R. & Choene, M. S. Antitumor effect of Iso-mukaadial acetate on MCF-7 breast cancer mice xenograft model. *Sci. Rep.* **14** (1), 13744. https://doi.org/10.1038/s41598-024-64474-x (2024).
11. Drewes, S. E., Crouch, N. R., Mashimbye, M. J., Leeuw, B. M. & De, Horn, M. M. A phytochemical basis for the potential use of Warburgia salutaris (pepper-bark tree) leaves in the place of bark.South African. *J. Sci.* **97** (9), 383–386 (2001).
12. Wube, A. A., Bucar, F., Gibbons, S. & Asres, K. Sesquiterpenes from *Warburgia ugandensis* and their antimycobacterial activity. *Phytochemistry* **66**(19), 2309–2315. https://doi.org/10.1016/j.phytochem.2005.07.018 (2005).
13. Tajuddeen, N. & Van Heerden, F. R. Antiplasmodial natural products: an update. *Malar. J.* **18** (1), 404. https://doi.org/10.1186/s12936-019-3026-1 (2019).
14. Cowman, A. F., Healer, J., Marapana, D., Marsh, K. & Malaria *Biology Disease Cell.* ;**167**(3):610–624. https://doi.org/10.1016/j.cell.2016.07.055 (2016).
15. Flannery, E. L., Chatterjee, A. K. & Winzeler, E. A. Antimalarial drug discovery-approaches and progress towards new medicines. *Nat. Rev. Microbiol.* **12** (12), 849–862. https://doi.org/10.1038/nrmicro3138 (2013).
16. Lee, H. J. et al. Transcriptomic studies of malaria: a paradigm for investigation of systemic Host-Pathogen interactions. *Microbiol. Mol. Biol. Rev.* **82** (2), e00071–e00017. https://doi.org/10.1128/MMBR.00071-17 (2018).
17. Nirmalan, N., Sims, P. F. G. & Hyde, J. E. Quantitative proteomics of the human malaria parasite plasmodium falciparum and its application to studies of development and Inhibition. *Mol. Microbiol.* **52** (4), 1187–1199. https://doi.org/10.1111/j.1365-2958.2004.04049.x (2004).
18. Sims, P. F. G. & Hyde, J. E. Proteomics of the human malaria parasite plasmodium falciparum. *Expert Rev. Proteom.* **3** (1), 87–95. https://doi.org/10.1586/14789450.3.1.87 (2006).
19. Alberts, B. et al. Molecular biology of the cell: Studying gene expression and function. *Garl. Sci.* 4 (2002). https://www.ncbi.nlm.nih.gov/books/NBK26818/
20. Pascual-Ahuir, A., Fita-Torró, J. & Proft, M. Capturing and Understanding the dynamics and heterogeneity of gene expression in the living cell. *Int. J. Mol. Sci.* **21** (21), 8278. https://doi.org/10.3390/ijms21218278 (2020).
21. Makler, M. T. & Hinrichs, D. J. Measurement of the lactate dehydrogenase activity of plasmodium falciparum as an assessment of parasitemia. *Am. J. Trop. Med. Hyg.* **48** (2), 205–210. https://doi.org/10.4269/ajtmh.1993.48.205 (1993).
22. Ponts, N., Chung, D. W. D. & Le Roch, K. G. Strand-specific RNA-seq applied to malaria samples. *Methods Mol. Biol.* **883**, 59–73. https://doi.org/10.1007/978-1-61779-839-9_4 (2012).
23. Andrews, S. FastQC - A quality control tool for high throughput sequence data. Babraham Bioinforma. (2010). http://www.bioinformatics.babraham.ac.uk/projects/fastqc/
24. Bolger, A. M., Lohse, M., Usadel, B. & Trimmomatic A flexible trimmer for illumina sequence data. *Bioinformatics* **30** (15), 2114–2120. https://doi.org/10.1093/bioinformatics/btu170 (2014).
25. Kim, D., Langmead, B. & Salzberg, S. L. HISAT: A fast spliced aligner with low memory requirements. *Nat. Methods*. **12** (4), 357–370. https://doi.org/10.1038/nmeth.3317 (2015).
26. Etherington, G. J., Ramirez-Gonzalez, R. H. & MacLean, D. Bio-samtools 2: A package for analysis and visualization of sequence and alignment data with samtools in Ruby. *Bioinformatics* **31** (1), 2565–2567. https://doi.org/10.1093/bioinformatics/btv178 (2015).
27. Danecek, P. et al. SAMtools. *Gigascience* **10**(2), giab008. https://doi.org/10.1093/gigascience/giab008 (2021).
28. Liao, Y., Smyth, G. K. & Shi, W. FeatureCounts: an efficient general purpose program for assigning sequence reads to genomic features. *Bioinformatics* **30** (7), 923–930. https://doi.org/10.1093/bioinformatics/btt656 (2014).
29. Love, M. I., Huber, W. & Anders, S. Moderated Estimation of fold change and dispersion for RNA-seq data with DESeq2. *Genome Biol.* **15** (12), 550. https://doi.org/10.1186/s13059-014-0550-8 (2024).
30. Cheng, C. & Pounds, S. False discovery rate paradigms for statistical analyses of microarray gene expression data. *Bioinformation* **1** (10), 436–446. https://doi.org/10.6026/97320630001436 (2007).
31. Stephens, M. False discovery rates: A new deal. *Biostatistics* **18** (2), 275–294. https://doi.org/10.1093/biostatistics/kxw041 (2017).
32. Ge, S. X., Jung, D., Jung, D. & Yao, R. ShinyGO: A graphical gene-set enrichment tool for animals and plants. *Bioinformatics* **36** (8), 2628–2629. https://doi.org/10.1093/bioinformatics/btz931 (2020).
33. Kolberg, L. et al. G:Profiler-interoperable web service for functional enrichment analysis and gene identifier mapping (2023 update). *Nucleic Acids Res.* **51** (W1), W207–W212. https://doi.org/10.1093/nar/gkad347 (2023).
34. Aurrecoechea, C. et al. PlasmoDB: A functional genomic database for malaria parasites. *Nucleic Acids Res.* **37**, D539–543. https://doi.org/10.1093/nar/gkn814 (2009).
35. Lasonder, E. et al. Integrated transcriptomic and proteomic analyses of P. Falciparum gametocytes: molecular insight into sex-specific processes and translational repression. *Nucleic Acids Res.* **44** (13), 6087–6101. https://doi.org/10.1093/nar/gkw536 (2016).
36. Clarkson, C. et al. In vitro antiplasmodial activity of medicinal plants native to or naturalised in South Africa. *J. Ethnopharmacol.* **92** (2-3), 177–191. https://doi.org/10.1016/j.jep.2004.02.011 (2004).
37. Bathurst, I. & Hentschel, C. Medicines for malaria venture: sustaining antimalarial drug development. *Trends Parasitol.* **22** (7), 301–307. https://doi.org/10.1016/j.pt.2006.05.011 (2006).

38. Samby, K., Willis, P. A., Burrows, J. N., Laleu, B. & Webborn, P. J. H. Actives from MMV open access boxes? A suggested way forward. *PLoS Pathog.* **17** (4), e1009384. https://doi.org/10.1371/journal.ppat.1009384 (2021).
39. Pawitan, Y., Michiels, S., Koscielny, S., Gusnanto, A. & Ploner, A. False discovery rate, sensitivity and sample size for microarray studies. *Bioinformatics* **21** (13), 3017–3024. https://doi.org/10.1093/bioinformatics/bti448 (2005).
40. Chen, X., Robinson, D. G. & Storey, J. D. The functional false discovery rate with applications to genomics. *Biostatistics* **22** (1), 68–81. https://doi.org/10.1093/biostatistics/kxz010 (2021).
41. Siavoshi, A., Taghizadeh, M., Dookhe, E. & Piran, M. Gene expression profiles and pathway enrichment analysis to identification of differentially expressed gene and signaling pathways in epithelial ovarian cancer based on high-throughput RNA-seq data. *Genomics* **114** (1), 161–170. https://doi.org/10.1016/j.ygeno.2021.11.031 (2022).
42. Dalmer, T. R. A. & Clugston, R. D. Gene ontology enrichment analysis of congenital diaphragmatic hernia-associated genes. *Pediatr. Res.* **85** (1), 13–19. https://doi.org/10.1038/s41390-018-0192-8 (2019).
43. Thomas, P. D. The gene ontology and the meaning of biological function. *Methods Mol. Biol.* **1446**, 15–24. https://doi.org/10.1007/978-1-4939-3743-1_2 (2017).
44. Reimand, J. et al. Pathway enrichment analysis and visualization of omics data using g:Profiler, GSEA, cytoscape and enrichment map. *Nat. Protoc.* **14** (2), 482–517. https://doi.org/10.1038/s41596-018-0103-9 (2019).
45. Lee, W. C., Russell, B. & Rénia, L. Sticking for a cause: the falciparum malaria parasites cytoadherence paradigm. *Front. Immunol.* **10**, 1444. https://doi.org/10.3389/fimmu.2019.01444 (2019).
46. Chan, J. A., Fowkes, F. J. I. & Beeson, J. G. Surface antigens of plasmodium falciparum-infected erythrocytes as immune targets and malaria vaccine candidates. *Cell. Mol. Life Sci.* **71** (19), 3633–3657. https://doi.org/10.1007/s00018-014-1614-3 (2014).
47. Molina-Franky, J., Patarroyo, M. E., Kalkum, M. & Patarroyo, M. A. The cellular and molecular interaction between erythrocytes and plasmodium falciparum merozoites. *Front. Cell. Infect. Microbiol.* **12**, 816574. https://doi.org/10.3389/fcimb.2022.816574 (2022).
48. Belachew, E. B. Immune response and evasion mechanisms of plasmodium falciparum parasites. *J. Immunol. Res.* **2018**, 6529681. https://doi.org/10.1155/2018/6529681 (2018).
49. Salanti, A. et al. Selective upregulation of a single distinctly structured var gene in chondroitin sulphate A-adhering plasmodium falciparum involved in pregnancy-associated malaria. *Mol. Microbiol.* **49**, 179–191. https://doi.org/10.1046/j.1365-2958.2003.03570.x (2003).
50. Bull, P. C. & Abdi, A. I. The role of PfEMP1 as targets of naturally acquired immunity to childhood malaria: prospects for a vaccine. *Parasitology* **143** (2), 171–186. https://doi.org/10.1017/S0031182015001274 (2016).
51. Mwakalinga, S. B. et al. Expression of a type B RIFIN in plasmodium falciparum merozoites and gametes. *Malar. J.* **11**, 429. https://doi.org/10.1186/1475-2875-11-429 (2012).
52. Niang, M. et al. STEVOR is a plasmodium falciparum erythrocyte binding protein that mediates merozoite invasion and rosetting. *Cell. Host Microbe.* **16** (1), 81–93. https://doi.org/10.1016/j.chom.2014.06.004 (2014).
53. Lopaticki, S. et al. Reticulocyte and erythrocyte binding-like proteins function cooperatively in invasion of human erythrocytes by malaria parasites. *Infect. Immun.* **79** (3), 1107–1117. https://doi.org/10.1128/IAI.01021-10 (2011).
54. Maier, A. G., Baum, J., Smith, B., Conway, D. J. & Cowman, A. F. Polymorphisms in erythrocyte binding antigens 140 and 181 affect function and binding but not receptor specificity in plasmodium falciparum. *Infect. Immun.* **77** (4), 1689–1699. https://doi.org/10.1128/IAI.01331-08 (2009).
55. Dunyak, B. M. & Gestwicki, J. E. Peptidyl-Proline isomerases (PPIases): targets for natural products and natural Product-Inspired compounds. *J. Med. Chem.* **59** (21), 9622–9644. https://doi.org/10.1021/acs.jmedchem.6b00411 (2016).
56. Aranda-Chan, V. et al. Insights into Peptidyl-Prolyl cis-trans isomerases from clinically important protozoans: from structure to potential biotechnological applications. *Pathogens* **13** (8), 644. https://doi.org/10.3390/pathogens13080644 (2024).
57. Gurung, D. et al. Proline isomerization: from the chemistry and biology to therapeutic opportunities. *Biology (Basel).* **12** (7), 1008. https://doi.org/10.3390/biology12071008 (2023).
58. Fisher, G. M. et al. The key glycolytic enzyme phosphofructokinase is involved in resistance to antiplasmodial glycosides. *MBio* **11** (6), e02842–e02820. https://doi.org/10.1128/mBio.02842-20 (2020).
59. Gemayel, R. Malaria, metabolism and mathematical models. *FEBS J.* **284** (16), 2553–2555. https://doi.org/10.1111/febs.14161 (2017).
60. Tewari, S. G., Prigge, S. T., Reifman, J. & Wallqvist, A. Using a genome-scale metabolic network model to elucidate the mechanism of chloroquine action in plasmodium falciparum. *Int. J. Parasitol. Drugs Drug Resist.* **7** (2), 138–146. https://doi.org/10.1016/j.ijpddr.2017.03.004 (2017).
61. Ishii, R., Sakura, T., Inaoka, D. K. & Tokumasu, F. Glycolytic enzymes form membrane-less condensates in the malaria parasite *Plasmodium falciparum* by sensing glucose levels. bioRxiv. Available from: https://www.biorxiv.org/content/ (2024). https://doi.org/10.1101/2024.04.08.588540v3
62. Avilán, L. et al. Enolase: A key player in the metabolism and a probable virulence factor of trypanosomatid parasites - Perspectives for its use as a therapeutic target. *Enzyme Res.* **2011**, 932549. https://doi.org/10.4061/2011/932549 (2011).
63. Krause, R. G. E. et al. Plasmodium glyceraldehyde-3-phosphate dehydrogenase: A potential malaria diagnostic target. *Exp. Parasitol.* **179**, 7–19. https://doi.org/10.1016/j.exppara.2017.05.007 (2017).
64. Abadio, A. K. R. et al. A pharmacophore-based virtual screening approach for the discovery of trypanosoma Cruzi GAPDH inhibitors. *J. Chem. Inf. Model.* **5**, 2013–2019 (2015).
65. Ayi, K. et al. Pyruvate kinase deficiency and malaria. *N Engl. J. Med.* **358** (17), 1805–1810. https://doi.org/10.1056/NEJMoa072464 (2008).
66. Zhong, W. et al. Pyruvate kinase from plasmodium falciparum: structural and kinetic insights into the allosteric mechanism. *Biochem. Biophys. Res. Commun.* **532** (3), 370–376. https://doi.org/10.1016/j.bbrc.2020.08.048 (2020).
67. Padín-Irizarry, V. et al. Glutathione-deficient plasmodium Berghei parasites exhibit growth delay and nuclear DNA damage. *Free Radic Biol. Med.* **95**, 43–54. https://doi.org/10.1016/j.freeradbiomed.2016.02.032 (2016).
68. Bhattacharya, S. et al. RAD51 interconnects between DNA replication, DNA repair and immunity. *Nucleic Acids Res.* **45** (8), 4590–4605. https://doi.org/10.1093/nar/gkx126 (2017).
69. Singh, P., Rani, K., Gotmare, A. & Bhattacharyya, S. A Tale of topoisomerases and the Knotty genetic material in the backdrop of plasmodium biology. *Biosci. Rep.* **42** (6), BSR20212847. https://doi.org/10.1042/BSR20212847 (2022).
70. Absalon, S. & Dvorin, J. D. Depletion of the mini-chromosome maintenance complex binding protein allows the progression of cytokinesis despite abnormal karyokinesis during the asexual development of plasmodium falciparum. *Cell. Microbiol.* **23** (3), e13284. https://doi.org/10.1111/cmi.13284 (2021).
71. Saldanha, J., Rageul, J., Patel, J. A. & Kim, H. The adaptive mechanisms and checkpoint responses to a stressed DNA replication fork. *Int. J. Mol. Sci.* **24** (13), 10488. https://doi.org/10.3390/ijms241310488 (2023).
72. Costa-Silva, H. M. et al. DNA Topoisomerase 3α is involved in homologous recombination repair and replication stress response in *Trypanosoma cruzi*. *Front Cell Dev Biol.* **9**, 633195w. https://doi.org/10.3389/fcell.2021.633195 (2021).
73. Jedrychowska, M. et al. Defects in the GINS complex increase the instability of repetitive sequences via a recombination-dependent mechanism. *PLoS Genet.* **15** (12), e1008494. https://doi.org/10.1371/journal.pgen.1008494 (2019).
74. Marinsek, N. et al. GINS, a central nexus in the archaeal DNA replication fork. *EMBO Rep.* **7** (5), 539–545. https://doi.org/10.1038/sj.embor.7400649 (2006).

75. Dueva, R. & Iliakis, G. Replication protein A: a multifunctional protein with roles in DNA replication, repair and beyond. *NAR Cancer*. **2** (3), zcaa022. https://doi.org/10.1093/narcan/zcaa022 (2020).
76. Kirkman, L. A., Lawrence, E. A. & Deitsch, K. W. Malaria parasites utilize both homologous recombination and alternative end joining pathways to maintain genome integrity. *Nucleic Acids Res.* **42** (1), 370–379. https://doi.org/10.1093/nar/gkt881 (2014).
77. Tuteja, R. Unraveling the importance of the malaria parasite helicases. *FEBS J.* **284** (16), 2592–2603. https://doi.org/10.1111/febs.14109 (2017).
78. Spillman, N. J., Beck, J. R., Ganesan, S. M., Niles, J. C. & Goldberg, D. E. The chaperonin TRiC forms an oligomeric complex in the malaria parasite cytosol. *Cell. Microbiol.* https://doi.org/10.1111/cmi.12719 (2017).
79. Saibil, H. Chaperone machines for protein folding, unfolding and disaggregation. *Nat. Rev. Mol. Cell. Biol.* **14** (10), 630–642. https://doi.org/10.1038/nrm3658 (2013).
80. Wilkes, J. M. & Doerig, C. The protein-phosphatome of the human malaria parasite plasmodium falciparum. *BMC Genom.* **9**, 412. https://doi.org/10.1186/1471-2164-9-412 (2008).
81. Fréville, A. et al. Deciphering the role of protein phosphatases in apicomplexa: the future of innovative. *Therapeutics? Microorganisms*. **10** (3), 585. https://doi.org/10.3390/microorganisms10030585 (2022).
82. Priya, P. P., Grover, M., Tatu, U. S., Natarajan, V. & Langsley, G. Characterization of precursor PfHsp60 in plasmodium falciparum cytosol during its asexual development in human erythrocytes. *PLoS One*. **10** (8), e0136401. https://doi.org/10.1371/journal.pone.0136401 (2015).
83. Lu, K. Y. et al. Plasmodium chaperonin TRiC/CCT identified as a target of the antihistamine clemastine using parallel chemoproteomic strategy. *Proc. Natl. Acad. Sci. U S A*. **117** (11), 5810–5817. https://doi.org/10.1073/pnas (2020).
84. Timothy, F. M. & Zininga, T. Small heat shock proteins as modulators of cell death in *Plasmodium falciparum* parasites and its human host. *Front. Cell. Death* https://doi.org/10.3389/fceld.2023.1322780 (2023).
85. Shankar, K. & Mehendale, H. M. Heat-shock proteins. *Encycl Toxicol. Third Ed.* **3**, 830–831. https://doi.org/10.1016/B978-0-12-386454-3.00320-1 (2014).
86. Przyborski, J. M., Diehl, M. & Blatch, G. L. Plasmodial HSP70s are functionally adapted to the malaria parasite life cycle. *Front. Mol. Biosci.* **2**, 34. https://doi.org/10.3389/fmolb.2015.00034 (2015).
87. Assimon, A., Gillies, V. T., Rauch, A. N. & Gestwicki, J. E. Hsp70 protein complexes as drug targets. *Curr. Pharm. Des.* **19** (3), 404–417. https://doi.org/10.2174/138161213804143699 (2013).
88. Evans, C. G., Chang, L. & Gestwicki, J. E. Heat shock protein 70 (Hsp70) as an emerging drug target. *J. Med. Chem.* **53** (12), 4585–4602. https://doi.org/10.1021/jm100054f (2010).
89. Kapp, L. D. & Lorsch, J. R. The molecular mechanics of eukaryotic translation. *Annu. Rev. Biochem.* **73**, 657–704. https://doi.org/10.1146/annurev.biochem.73.030403.080419 (2004).
90. De Villiers, K. A. & Egan, T. J. Heme detoxification in the malaria parasite: A target for antimalarial drug development. *Acc. Chem. Res.* **54** (11), 2649–2659. https://doi.org/10.1021/acs.accounts.1c00154 (2021).
91. Chaudhari, R., Sharma, S. & Patankar, S. Glutathione and thioredoxin systems of the malaria parasite plasmodium falciparum: partners in crime? *Biochem. Biophys. Res. Commun.* **488** (1), 95–100. https://doi.org/10.1016/j.bbrc.2017.05.015 (2017).
92. Munte, C. E. & Kalbitzer, H. R. Solution structure and pressure response of thioredoxin-1 of plasmodium falciparum. *PLoS One*. **19** (4), e0301579. https://doi.org/10.1371/journal.pone.0301579 (2024).
93. McCarty, S. E. et al. Plasmodium falciparum thioredoxin reductase (PfTrxR) and its role as a target for new antimalarial discovery. *Molecules* **20** (6), 11459–11473. https://doi.org/10.3390/molecules200611459 (2015).
94. Kirk, K., Martin, R. E., Bröer, S., Howitt, S. M. & Saliba, K. J. Plasmodium permeomics: Membrane transport proteins in the malaria parasite. *Curr. Top. Microbiol. Immunol.* **295**, 325–356. https://doi.org/10.1007/3-540-29088-5_13 (2005).
95. Martin, R. E., Henry, R. I., Abbey, J. L., Clements, J. D. & Kirk, K. The permeome of the malaria parasite: an overview of the membrane transport proteins of plasmodium falciparum. *Genome Biol.* **6** (3), R26. https://doi.org/10.1186/gb-2005-6-3-r26 (2005).
96. Sanchez, C. P. et al. The Knock-Down of the chloroquine resistance transporter PfCRT is linked to oligopeptide handling in plasmodium falciparum. *Microbiol. Spectr.* **10** (4), e0110122. https://doi.org/10.1128/spectrum.01101-22 (2022).
97. Kanehisa, M. & Goto, S. KEGG: Kyoto encyclopedia of genes and genomes. *Nucleic Acids Res.* **28** (1), 27–30. https://doi.org/10.1093/nar/28.1.27 (2000).
98. Kanehisa, M., Furumichi, M., Sato, Y., Kawashima, M. & Ishiguro-Watanabe, M. KEGG for taxonomy-based analysis of pathways and genomes. *Nucleic Acids Res.* **51** (D1), D587–592. https://doi.org/10.1093/nar/gkac963 (2023).
99. Kanehisa, M. Toward Understanding the origin and evolution of cellular organisms. *Protein Sci.* **28** (11), 1947–1951. https://doi.org/10.1002/pro.3715 (2019).
100. McDonald, A. G. & Tipton, K. F. Enzyme nomenclature and classification: the state of the Art. *FEBS J.* **290** (9), 2214–2231. https://doi.org/10.1111/febs.16274 (2023).
101. Oyelade, J., Isewon, I., Rotimi, S. & Okunoren, I. Modeling of the Glycolysis pathway in plasmodium falciparum using petri Nets. *Bioinform Biol. Insights*. **10**, 49–57. https://doi.org/10.4137/BBI.S37296 (2016).
102. Michal, G. & Schomburg, D. Biochemical pathways: An Atlas of Biochemistry and Molecular Biology, Second Edition (2013).
103. Sharma, S., Jarori, G. K. & Sonawat, H. M. Glycolysis. *Encycl Malar.* 1–15 (2013).
104. Solebo, O. et al. Plasmodium falciparum utilizes pyrophosphate to fuel an essential proton pump in the ring stage and the transition to trophozoite stage. *PLoS Pathog*. **19** (12), e1011818. https://doi.org/10.1371/journal.ppat.1011818 (2023).
105. Olafsson, P., Matile, H. & Certa, U. Molecular analysis of plasmodium falciparum hexokinase. *Mol. Biochem. Parasitol.* **56** (1), 89–101. https://doi.org/10.1016/0166-6851(92)90157-f (1992).
106. Feng, J. et al. Emerging roles and the regulation of aerobic Glycolysis in hepatocellular carcinoma. *J. Exp. Clin. Cancer Res.* **39** (1), 126. https://doi.org/10.1186/s13046-020-01629-4 (2020).
107. Zuma, L. K. et al. Assessing the efficacy of iso-mukaadial acetate and betulinic acid against selected plasmodium falciparum glycolytic pathway proteins: in Silico and in vitro studies. *BMC Chem.* **19** (1), 16. https://doi.org/10.1186/s13065-025-01380-x (2025).
108. Parthasarathy, S., Eaazhisai, K., Balaram, H., Balaram, P. & Murthy, M. R. N. Structure of plasmodium falciparum Triose-phosphate Isomerase-2-Phosphoglycerate complex at 1.1-Å resolution. *J. Biol. Chem.* **278** (52), 52461–52470. https://doi.org/10.1074/jbc.M308525200 (2003).
109. Yang, J., Kalhan, S. C. & Hanson, R. W. What is the metabolic role of phosphoenolpyruvate carboxykinase? *J. Biol. Chem.* **284**, 27025–27029. https://doi.org/10.1074/jbc.R109.040543 (2009).
110. Shi, L. & Tu, B. P. Acetyl-CoA and the regulation of metabolism: mechanisms and consequences. *Curr. Opin. Cell. Biol.* **33**, 125–131. https://doi.org/10.1016/j.ceb.2015.02.003 (2015).
111. Van Niekerk, D. D., Penkler, G. P., Du Toit, F. & Snoep, J. L. Targeting Glycolysis in the malaria parasite plasmodium falciparum. *FEBS J.* **283** (4), 634–646. https://doi.org/10.1111/febs.13615 (2016).
112. Chaudhry, R., & Varacallo, M. Biochemistry Glycolysis. StatPearls. (2018). https://www.ncbi.nlm.nih.gov/books/NBK482303/
113. Kovářová, J. & Barrett, M. P. The Pentose phosphate pathway in parasitic trypanosomatids. *Trends Parasitol.* **32** (8), 622–634. https://doi.org/10.1016/j.pt.2016.04.010 (2016).
114. Olszewski, K. L. & Llinás, M. Central carbon metabolism of plasmodium parasites. *Mol. Biochem. Parasitol.* **175** (2), 95–103. https://doi.org/10.1016/j.molbiopara.2010.09.001 (2011).

115. Joshi, S. et al. Molecular cloning and characterization of plasmodium falciparum transketolase. *Mol. Biochem. Parasitol.* **160** (1), 32–41. https://doi.org/10.1016/j.molbiopara.2008.03.005 (2008).
116. Kovářová, J. et al. Deletion of transketolase triggers a stringent metabolic response in promastigotes and loss of virulence in amastigotes of leishmania Mexicana. *PLoS Pathog.* **14** (3), e1006953. https://doi.org/10.1371/journal.ppat.1006953 (2018).
117. Hove-Jensen, B. et al. Phosphoribosyl diphosphate (PRPP): Biosynthesis, Enzymology, Utilization, and metabolic significance. *Microbiol. Mol. Biol. Rev.* **81** (1), e00040–e00016. https://doi.org/10.1128/MMBR.00040-16 (2017).
118. Mantilla, B. S., Brown, N., Fiedler, D. & Docampo, R. Protein targets of inositol pyrophosphate (5-IP7) in the parasite *Trypanosoma cruzi*. *BioRxiv* https://doi.org/10.1101/2020.01.09.900860 (2020).
119. Hurbain, J., Thommen, Q., Anquez, F. & Pfeuty, B. Quantitative modeling of Pentose phosphate pathway response to oxidative stress reveals a cooperative regulatory strategy. *iScience* **25** (8), 104681. https://doi.org/10.1016/j.isci.2022.104681 (2022).
120. Mullarky, E. & Cantley, L. C. Diverting glycolysis to combat oxidative stress. *Innov Med.* https://doi.org/10.1007/978-4-431-55651-0_1 (2015).
121. Matthews, H., Duffy, C. W. & Merrick, C. J. Checks and balances? DNA replication and the cell cycle in plasmodium. *Parasites Vectors.* **11** (1), 216. https://doi.org/10.1186/s13071-018-2800-1 (2018).
122. Stincone, A. et al. The return of metabolism: biochemistry and physiology of the Pentose phosphate pathway. *Biol. Rev.* **90** (3), 927–963. https://doi.org/10.1111/brv.12140 (2015).
123. Stillman, B. Smart machines at the DNA replication fork. *Cell* **78** (5), 725–728. https://doi.org/10.1016/s0092-8674(94)90362-x (1994).
124. Mitra, P., Banu, K., Deshmukh, A. S., Subbarao, N. & Dhar, S. K. Functional dissection of proliferating-cell nuclear antigens (1 and 2) in human malarial parasite plasmodium falciparum: possible involvement in DNA replication and DNA damage response. *Biochem. J.* **470** (1), 115–129. https://doi.org/10.1042/BJ20150452 (2015).
125. Sheriff, O., Yaw, A., Lai, S. K., loo hooi linn, Sze, S. K. & Preiser, P. R. Plasmodium falciparum replication factor C subunit 1 is involved in genotoxic stress response. *Cell. Microbiol.* **23** (2), e13277. https://doi.org/10.1111/cmi.13277 (2021).
126. Essers, J. et al. Nuclear dynamics of PCNA in DNA replication and repair. *Mol. Cell. Biol.* **25** (21), 9350–9359. https://doi.org/10.1128/MCB.25.21.9350-9359.2005 (2005).
127. Overmeer, R. M. et al. Replication factor C recruits DNA polymerase δ to sites of nucleotide excision repair but is not required for PCNA recruitment. *Mol. Cell. Biol.* **30** (20), 4828–4839. https://doi.org/10.1128/MCB.00285-10 (2010).
128. Cassera, M. B., Zhang, Y., Hazleton, K. Z. & Schramm, V. L. Purine and pyrimidine pathways as targets in plasmodium falciparum. *Curr. Top. Med. Chem.* **11** (16), 2103–2115. https://doi.org/10.2174/156802611796575948 (2011).
129. Roy, S., Nagappa, L. K., Prahladarao, V. S. & Balaram, H. Kinetic mechanism of plasmodium falciparum hypoxanthine-guanine-xanthine phosphoribosyltransferase. *Mol. Biochem. Parasitol.* **204** (2), 111–120. https://doi.org/10.1016/j.molbiopara.2016.02.006 (2015).
130. Downie, M. J., Kirk, K., Mamoun, C. & Ben Purine salvage pathways in the intraerythrocytic malaria parasite plasmodium falciparum. *Eukaryot. Cell.* **7** (8), 1231–1237. https://doi.org/10.1128/EC.00159-08 (2008).
131. Opoku, F., Govender, P. P., Pooe, O. J. & Simelane, M. B. C. Evaluating iso-mukaadial acetate and ursolic acid acetate as plasmodium falciparum hypoxanthineguanine-xanthine phosphoribosyltransferase inhibitors. *Biomolecules* **9** (12), 861. https://doi.org/10.3390/biom9120861 (2019).

Acknowledgements

The authors would like to acknowledge the Agricultural Research Centre (ARC)- Biotechnology Platform for their support in RNA sequencing.

Author contributions

MS and TM conceptualized and funded the study. JSM, FA, OP and RvLZ provided ethical approval and reviewed the manuscript. TM and NS performed all the computational analyses. NS wrote the manuscript with input from all the coauthors.

Funding

Student funding under the National Research Foundation (NRF) of South Africa with grant UID: 131108.

Declarations

Competing interests

The authors declare no competing interests.

Additional information

Supplementary Information The online version contains supplementary material available at https://doi.org/10.1038/s41598-025-26347-9.

Correspondence and requests for materials should be addressed to M.S.

Reprints and permissions information is available at www.nature.com/reprints.

Publisher's note Springer Nature remains neutral with regard to jurisdictional claims in published maps and institutional affiliations.

Open Access This article is licensed under a Creative Commons Attribution-NonCommercial-NoDerivatives 4.0 International License, which permits any non-commercial use, sharing, distribution and reproduction in any medium or format, as long as you give appropriate credit to the original author(s) and the source, provide a link to the Creative Commons licence, and indicate if you modified the licensed material. You do not have permission under this licence to share adapted material derived from this article or parts of it. The images or other third party material in this article are included in the article's Creative Commons licence, unless indicated otherwise in a credit line to the material. If material is not included in the article's Creative Commons licence and your intended use is not permitted by statutory regulation or exceeds the permitted use, you will need to obtain permission directly from the copyright holder. To view a copy of this licence, visit http://creativecommons.org/licenses/by-nc-nd/4.0/.

© The Author(s) 2025